XMM-Newton's impact on Relativistic Astrophysics: Black Holes

28th Texas Symposium on Relativistic Astrophysics
13-18 December 2015
Geneva, Switzerland

Norbert Schartel
(XMM-Newton Project Scientist)

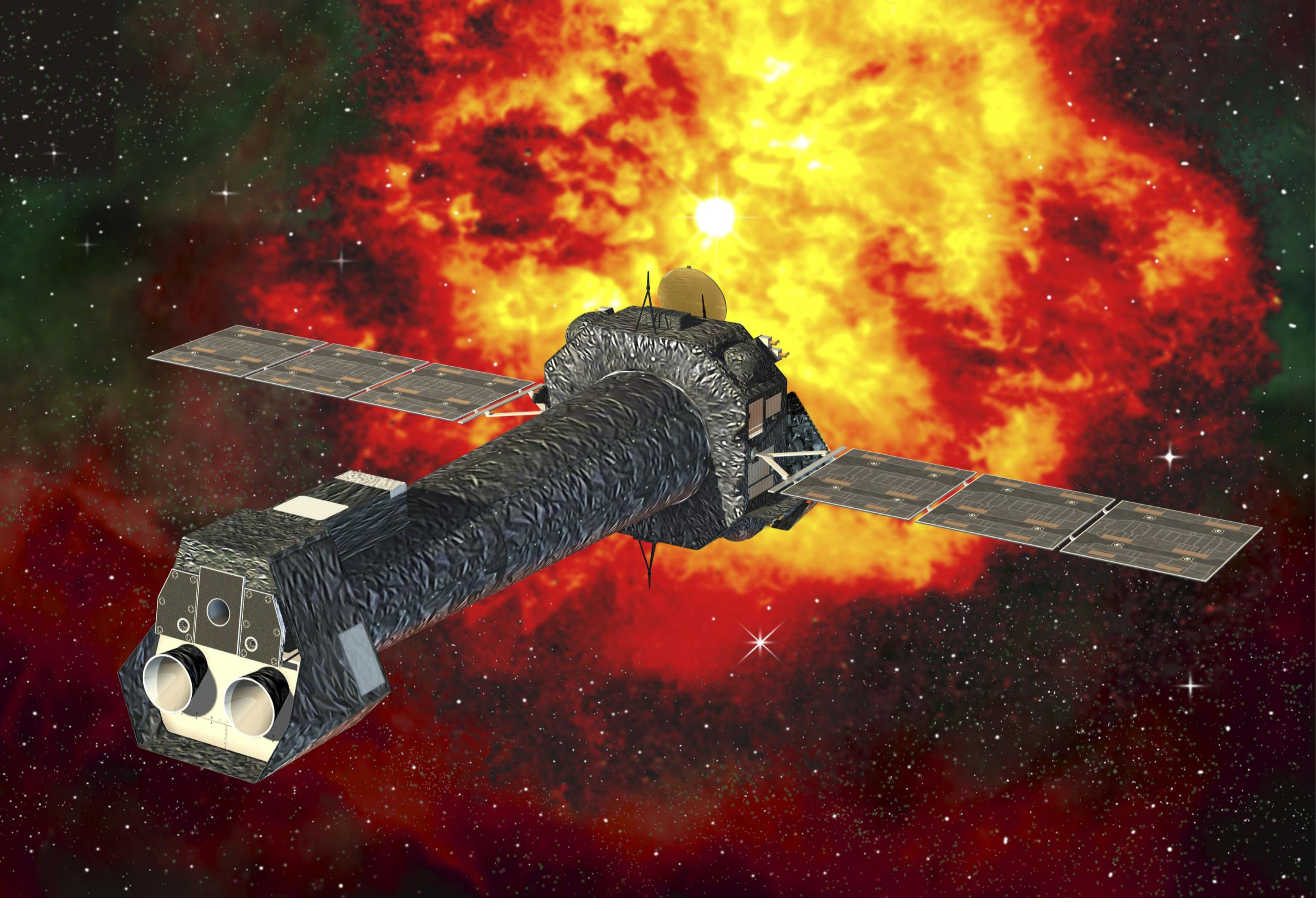

XMM-Newton preparation

Image courtesy of D. Parker

European Space Agency

Mirror Module:

- grazing-incidence Wolter 1 telescopes

- each mirror shell consists of a paraboloid and an associated hyperboloid

- 58 gold-coated nested mirrors

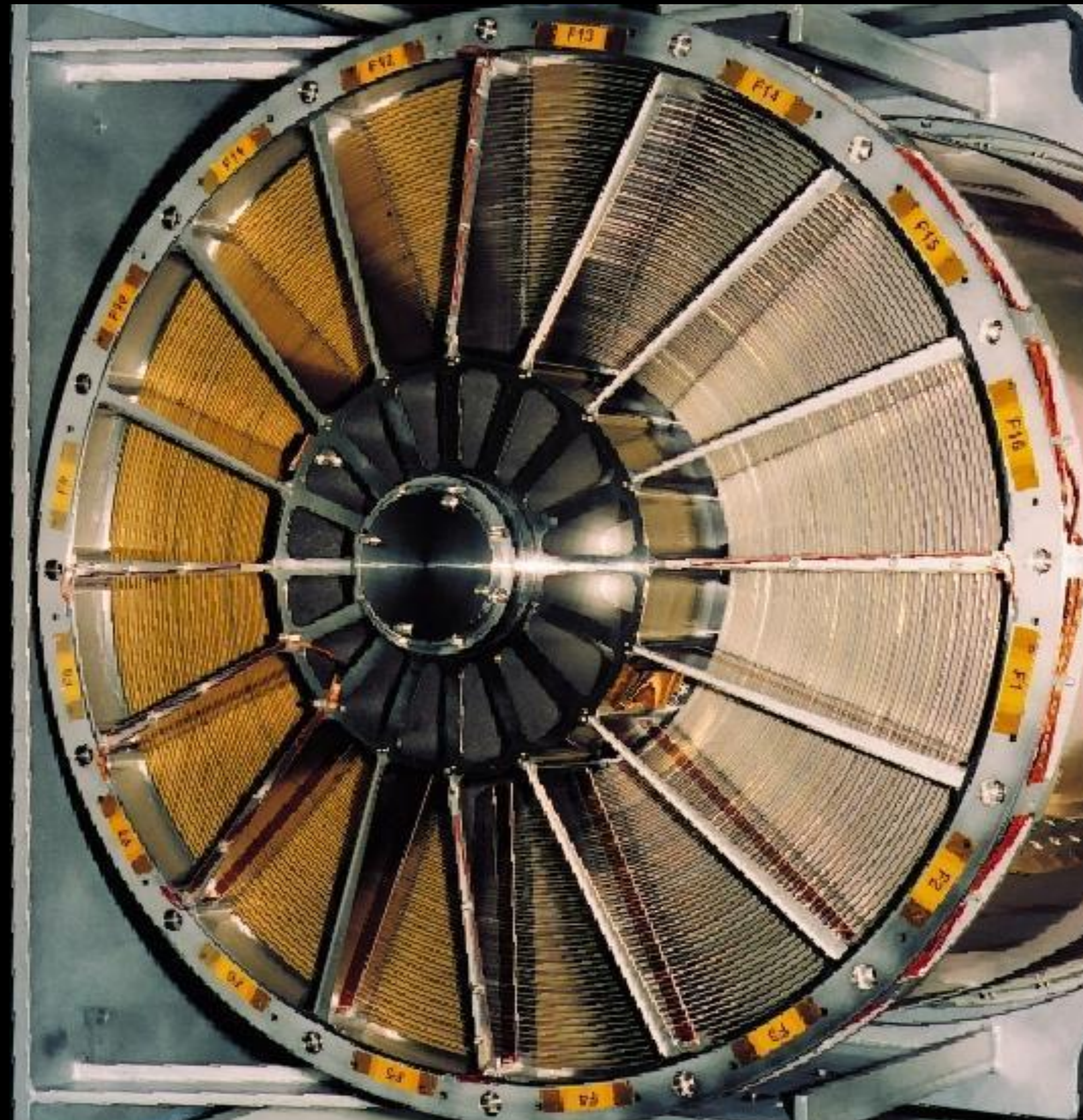

XMM-Newton mirrors during integration

Image courtesy of Dornier Satellitensysteme GmbH

European Space Agency

XMM-Newton has three mirror modules

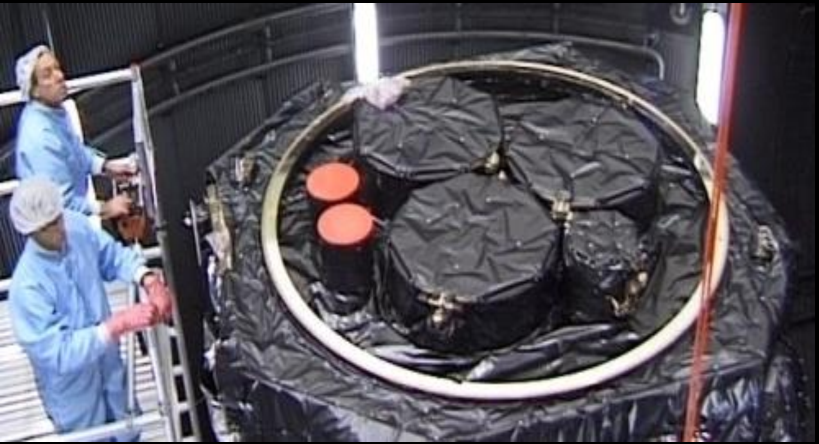

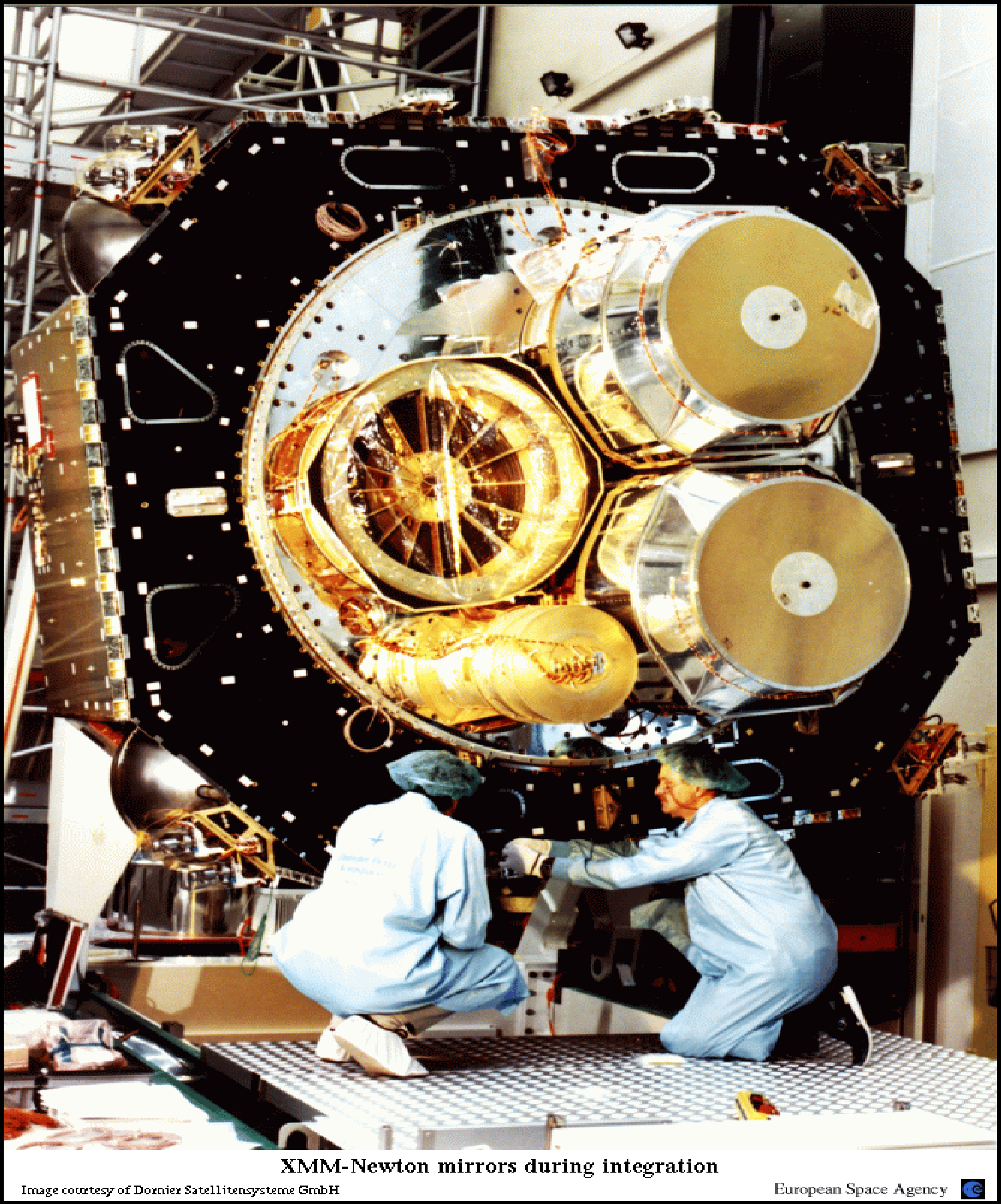

Instruments

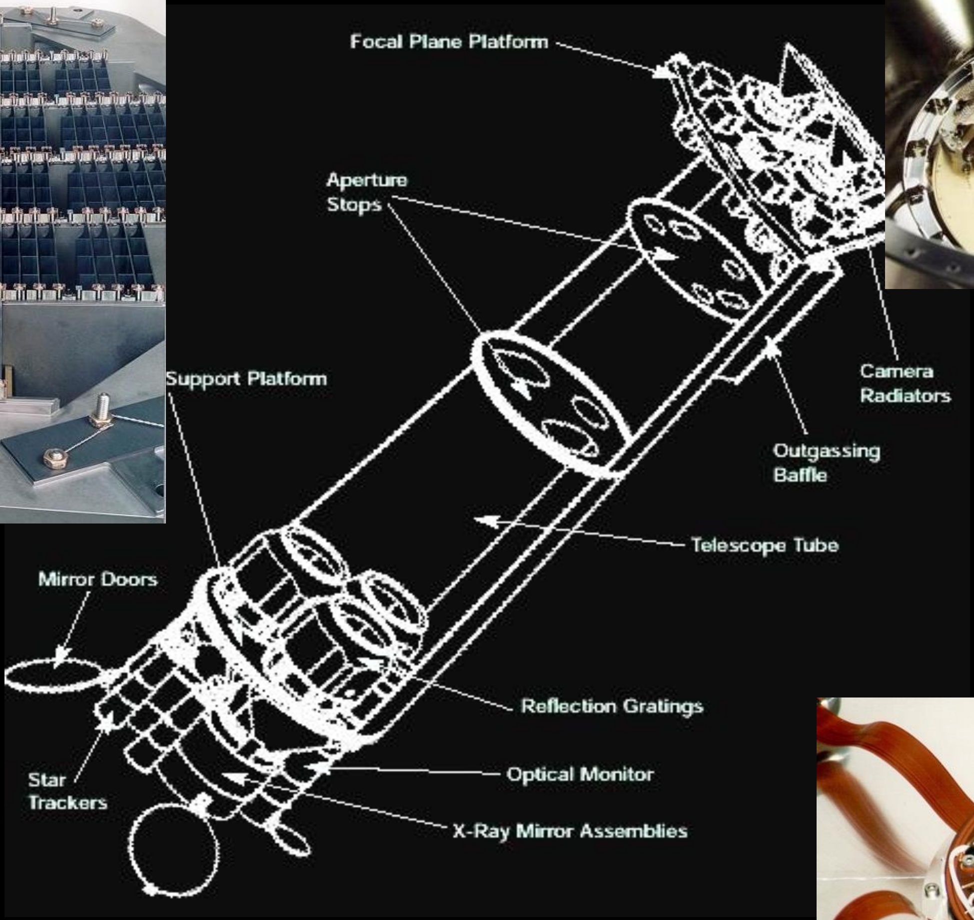

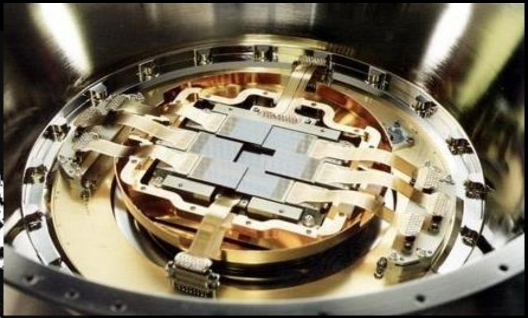

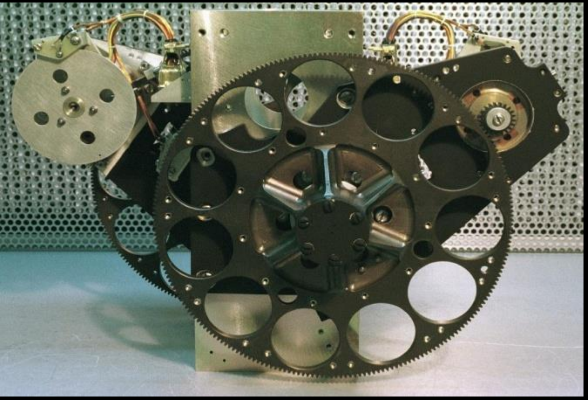

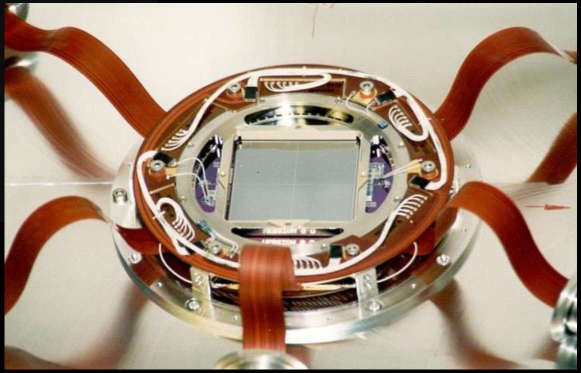

XMM-Newton

- 3 Mirror Modules / highest effective collecting area ever
- Six simultaneously observing instruments:
  - 3 CCD cameras (one pn and two MOSs)
  - 2 spectrometers (RGS)
  - 1 optical Monitor (OM)

GRB 031203 XMM–Newton observation

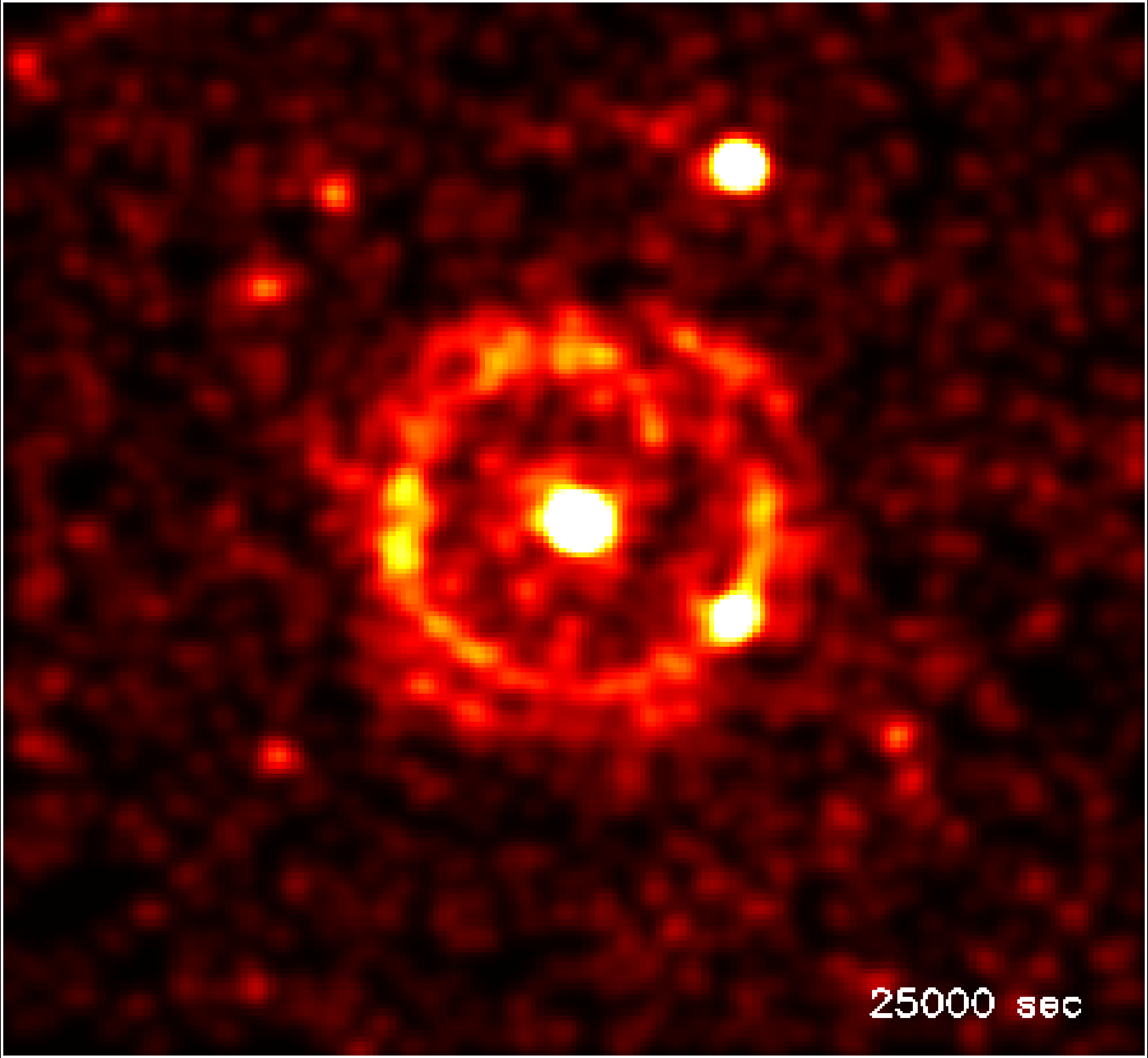

ESA, S. Vaughan (University of Leicester)

S. Vaughan et al., 2004, ApJ 603, L5

- ➔ Discovery of an evolving dust-scattered X-ray halo
- ➔ Will allow highly accurate distance determina-tions to the dust

Lord of the Rings: A Kinematic Distance to Circinus X-1 from a Giant X-Ray Light Echo

- Bright X-ray flare of Circinus X-1 in 2013.
- Follow-up observations with Chandra and XMM-Newton (40 & 80 days)

➔ bright X-ray light echo in the form of well-defined rings

➔ largest and brightest X-ray light echo observed to date

➔ distinct dust concentrations

➔ by comparing with CO maps of molecular clouds determination of the kinematic distance

$D_{CirX-1}=9.4\pm-0.9$ kpc.

➔ rules out earlier claims of ~4 kpc

➔ Circinus X-1 is a frequent super-Eddington source

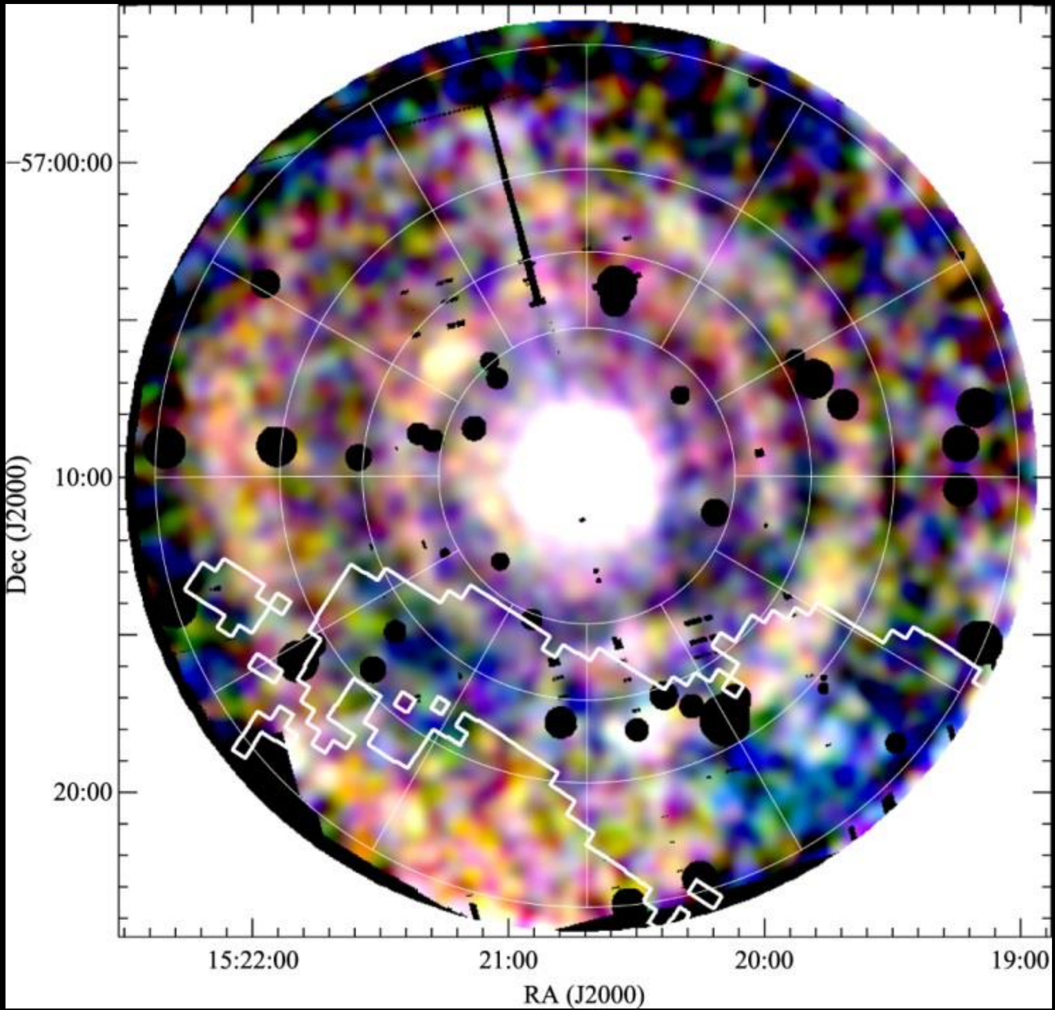

S. Heinz, et al., 2015, ApJ 806, 265

... ULX ...

First Black Hole In Globular Star Clusters

- GCs contain 10^3-10^6 old stars packed within tens of light years

➔ Formation of 10^3 solar mass BH ?

➔Interaction will eject BHs ?

T.J. Maccarone et al., 2007, Nature 445, 183

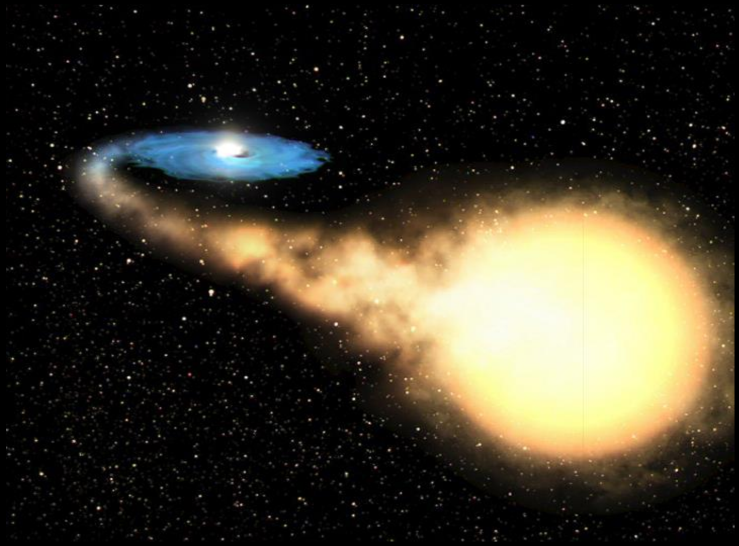

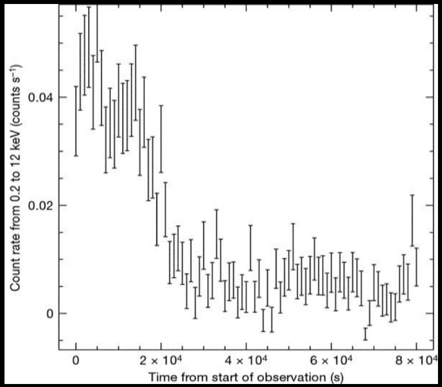

- X-ray source in GC associated with NGC 4472 (in the Virgo cluster)
- X-ray luminosity: 4×10^{39} erg s^{-1}
- Variability excludes composition by several objects

➔ Black hole (15-30 or 400 solar masses)

Baryons in the relativistic jets of the stellar-mass black-hole 4U 1630-47

- Accreting black holes power relativistic jets
- The power of the jets depends strongly on their composition
- Energetic considerations and circular-polarization measurements provide conflicting evidence for the presence or absence of baryons in jets (only exception peculiar X-ray binary SS 433)

➔ Detection of Doppler-shifted X-ray emission lines from a black-hole candidate X-ray binary 4U 1630-47

➔ Coincident with the reappearance of radio emission from the jets of the source

➔ Lines arise from baryonic matter in a jet travelling at ~2/3 speed of light, thereby establishing the presence of baryons in the jet

➔ Such baryonic jets are more likely to be powered by the accretion disk than by the spin of the black hole

M. Diaz Trigo et al., 2013, Nature 504, 260

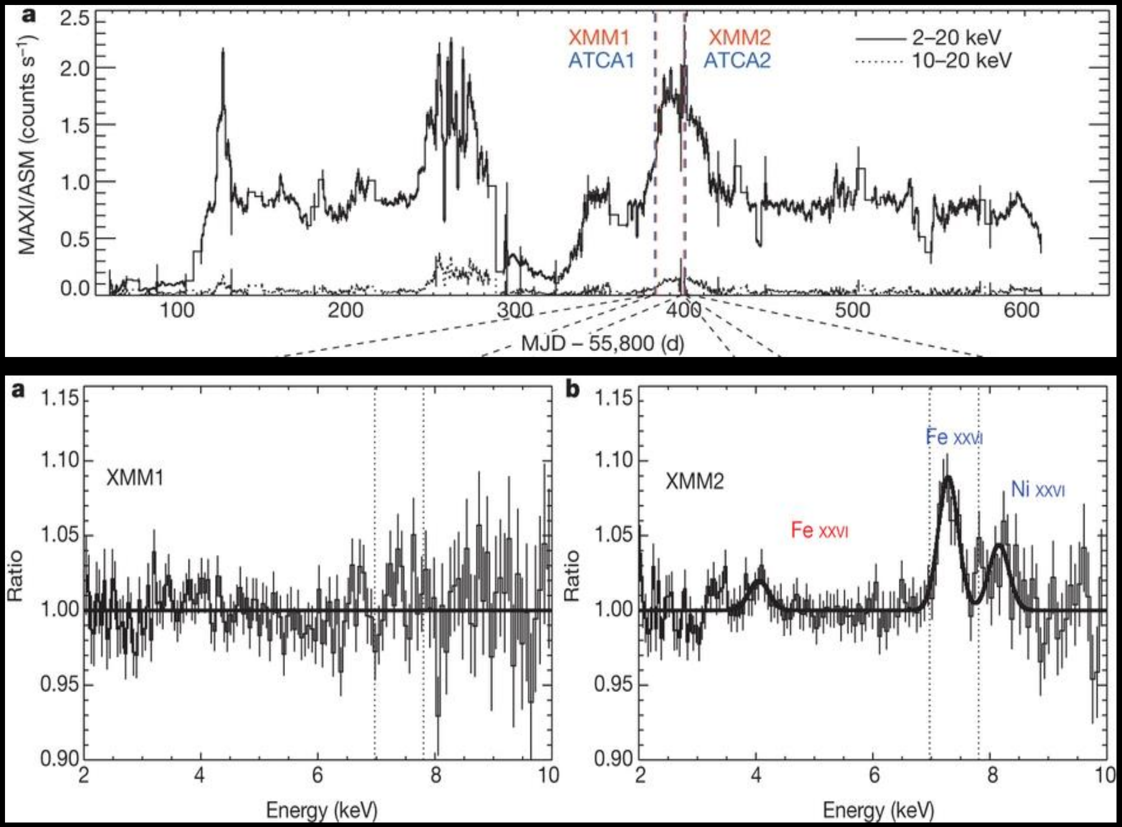

The first ultraluminous X-ray source (ULX) in M31

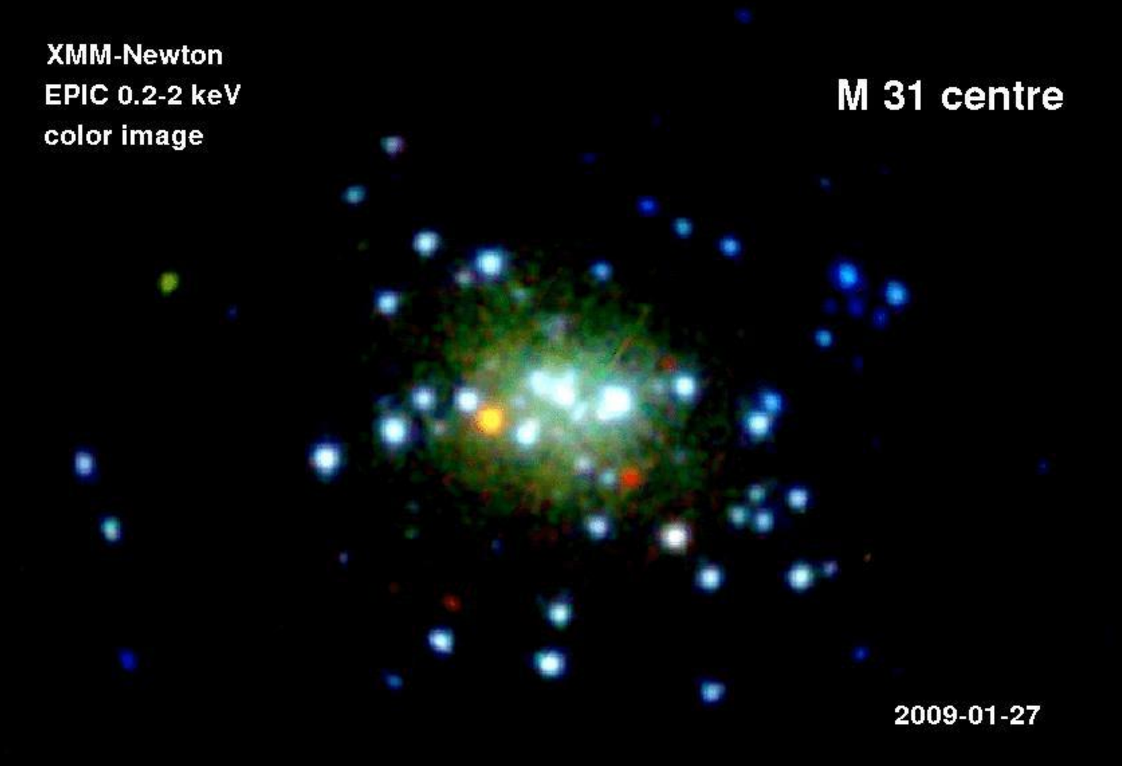

A. Kaur, et al., 2012, AA 538, 49

M. J. Middleton, et al., 2012, MNRAS 420 2969

- New, transient ultraluminous X-ray source (ULX) discovered by Chandra in M31 with a luminosity at ~5 × 10^{39} erg s^{-1}.
- 5 subsequent XMM-Newton observations show steady decline in X-ray luminosity over 1.5 months, from 1.8 × 10^{39} to 0.6 × 10^{39} erg s^{-1}

➔ Best sequence of high Eddington spectra ever assembled (low absorption & XMM-Newton)

- The spectra can be described by our best current disc model (10 M_{sun} black hole) or by a disc emission affected by advection & low-temperature Comptonization.

➔ Accretion on to a stellar mass black hole in a LMXB accreting in the Eddington regime.

➔ unambiguous connection of this object, and, by extension, similar low-luminosity ULXs, to 'standard' X-ray binaries.

XMMU J004243.6+412519: A ultraluminous X-ray source discovered in Andromeda

- XMM-Newton first detected XMMU J004243.6+412519 on 15 January 2012 at an X-ray luminosity of 2×10^{38} erg s^{-1}
- The source's location in an external galaxy allowed the astronomers to probe the emission both from the black hole's accretion disc, at X-ray wavelengths, and from its jets, in radio waves.

➔ These observations revealed, for the first time in an extragalactic stellar-mass black hole, the link between the source's X-ray brightening and the ejection of radio-bright material from the vicinity of the black hole into the jets, indicating an accretion rate close to the black hole's Eddington limit, or even above it.

M. Middleton et al., 2013, Nature 493, 187

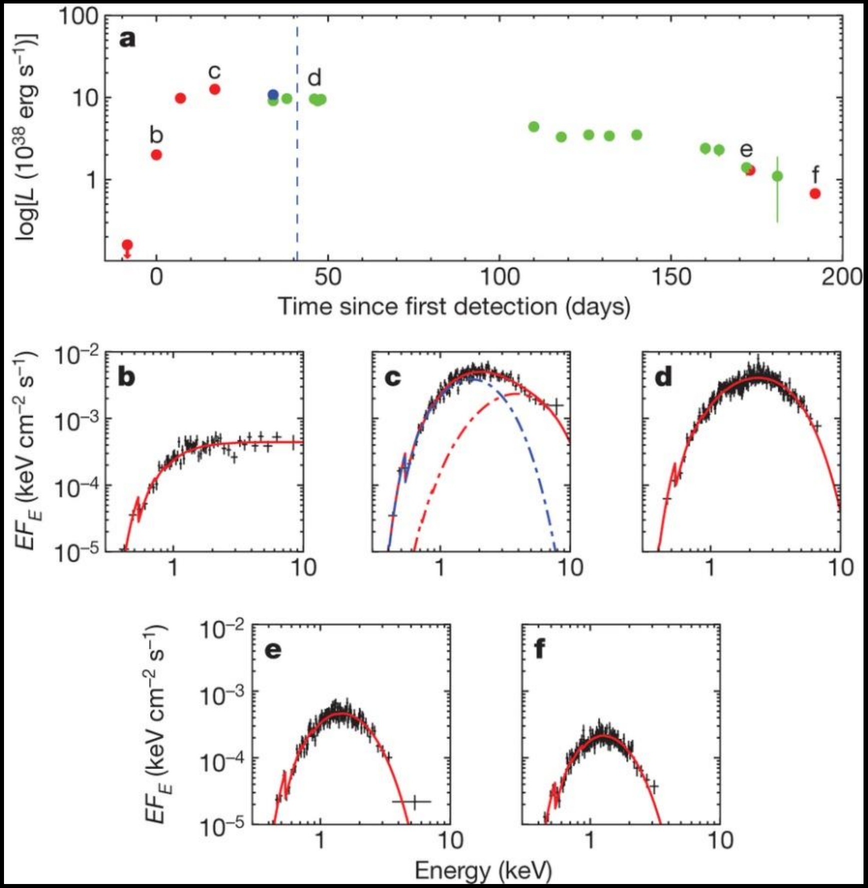

Evolution of the source brightness over ~200 days together with the time of the first VLA detection (blue vertical dashed line). The unabsorbed 0.3-10 keV luminosities are derived from the best-fitting models to the XMM-Newton observations (red), Chandra (blue) and Swift (green)

A mass of <15 solar masses for the black hole in an ultraluminous X-ray source in NGC 7793

- ULX have been interpreted either as intermediate-mass black holes (BH) or as stellar-mass BH accreting above their Eddington limit

- the ULX P13 in NGC 7793 is in a binary system with a period of 64 d

➔ strong optical/UV modulations are arising from X-ray heating of the B9Ia donor star and are allowing to constrain the BH mass <15 solar masses implying accretion above the Eddington limit

➔ by analogy, ULX with similar X-ray spectra and luminosities can be explained by super-Eddington accretion onto massive stellar-mass BH

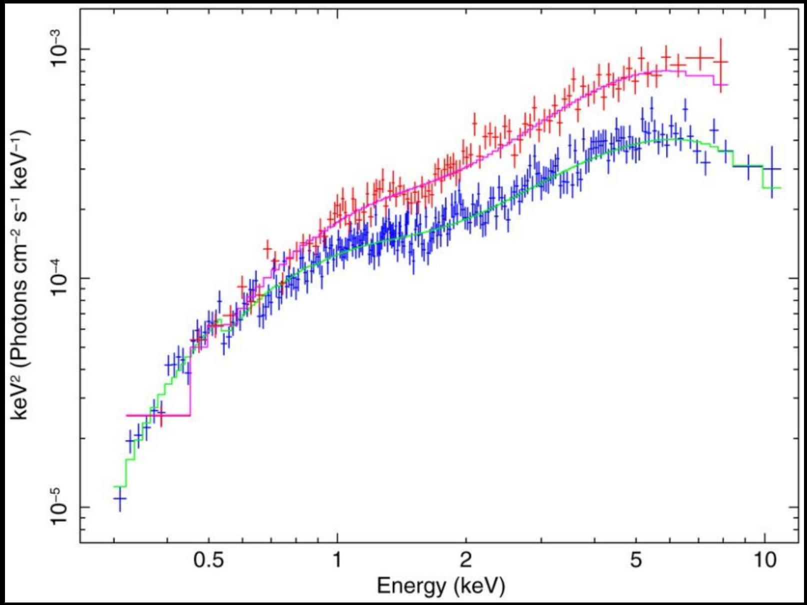

The E × f(E) unfolded energy distribution of the 2003 Chandra/ACIS-S (red) and of the 2013 XMM-Newton/EPIC (blue) fitted with a disk model.

C. Motch et al., 2014, Nature 514, 198

Ultraluminous X-Ray Source in NGC 1313

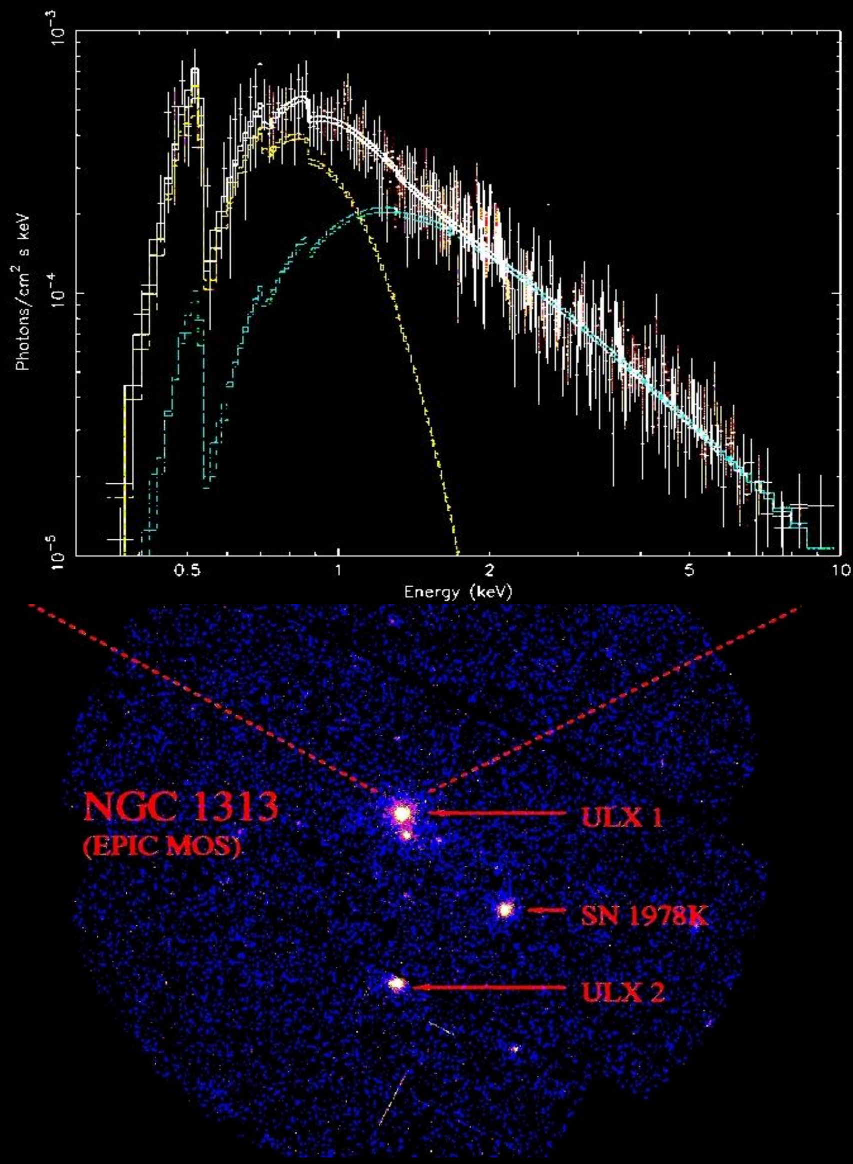

- Cool accretion disk (kT = 150 eV)
- ULX luminosity: 2.0 10^{40} ers/s

➔ BH mass 100-1000 MO

J. M. Miller et al., 2003, ApJ 585, 37

100 - 1000 solar masses

An Intermediate-Mass Black Hole In ESO 243-49

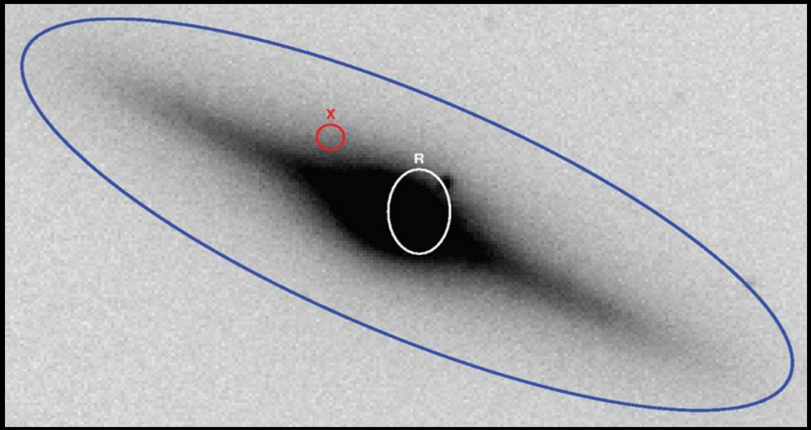

- 2XMM J011028.1-460421 identified in 2XMM Serendipitous Source catalogue
- Located in the edge-on spiral galaxy ESO 243-49 ➔ distance

S. A. Farrell, et al., 2009, Nature 460, 73

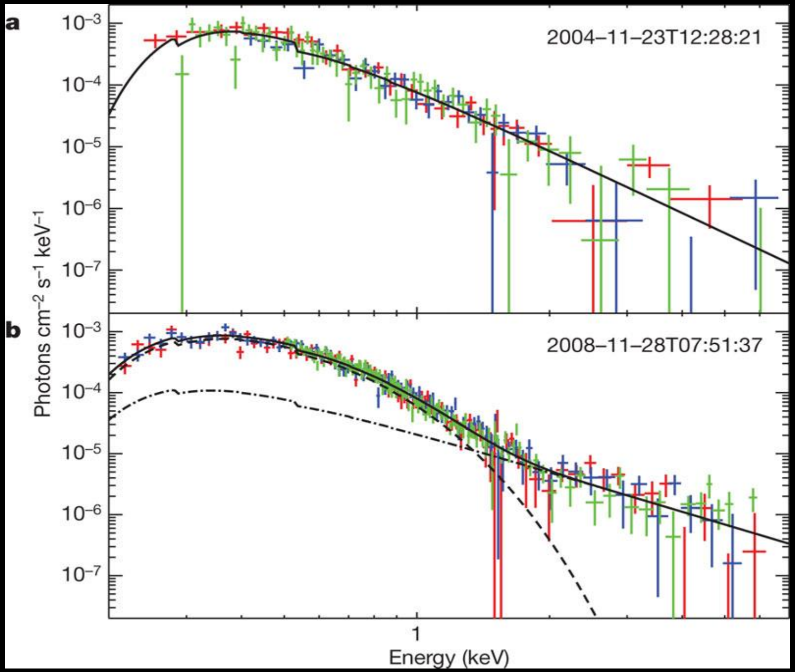

- Variability establishes:

➔ single source

➔ $L = 1.1 \times 10^{42}$ erg s^{-1}

➔ $m > 500\ M_o$

… Strong Gravitational Field …

Emission in the Strong Gravitational Field of the Black Hole

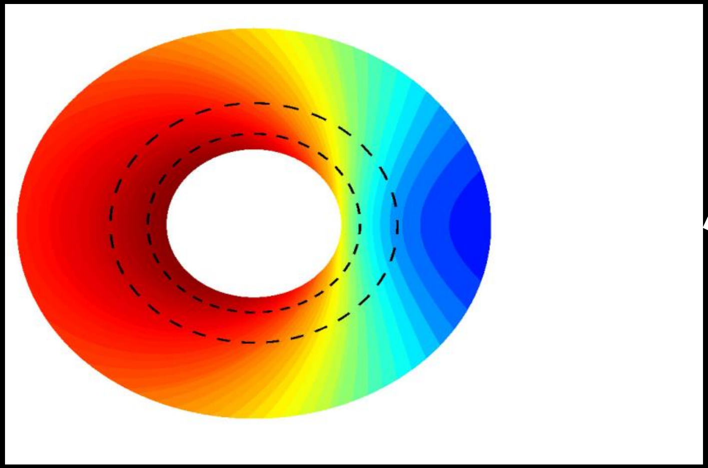

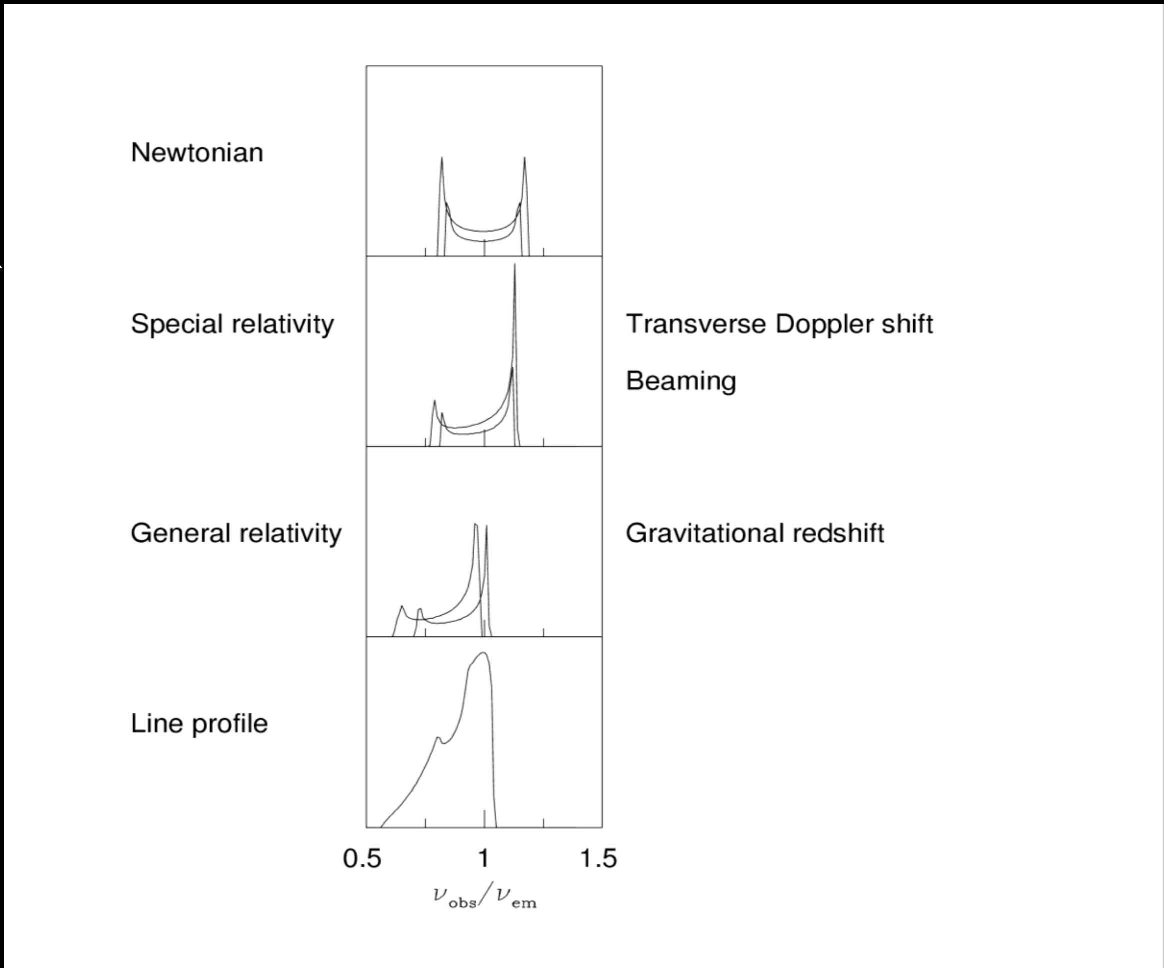

- Fabian et al. (1989); Laor et al (1990); Dovciak et al (2004); K. Beckwith & C. Done, Chris, 2005, MNRAS 359, 1217
- Image courtesy A. Fabian

Emission in the Strong Gravitational Field of the (Kerr) Black Hole

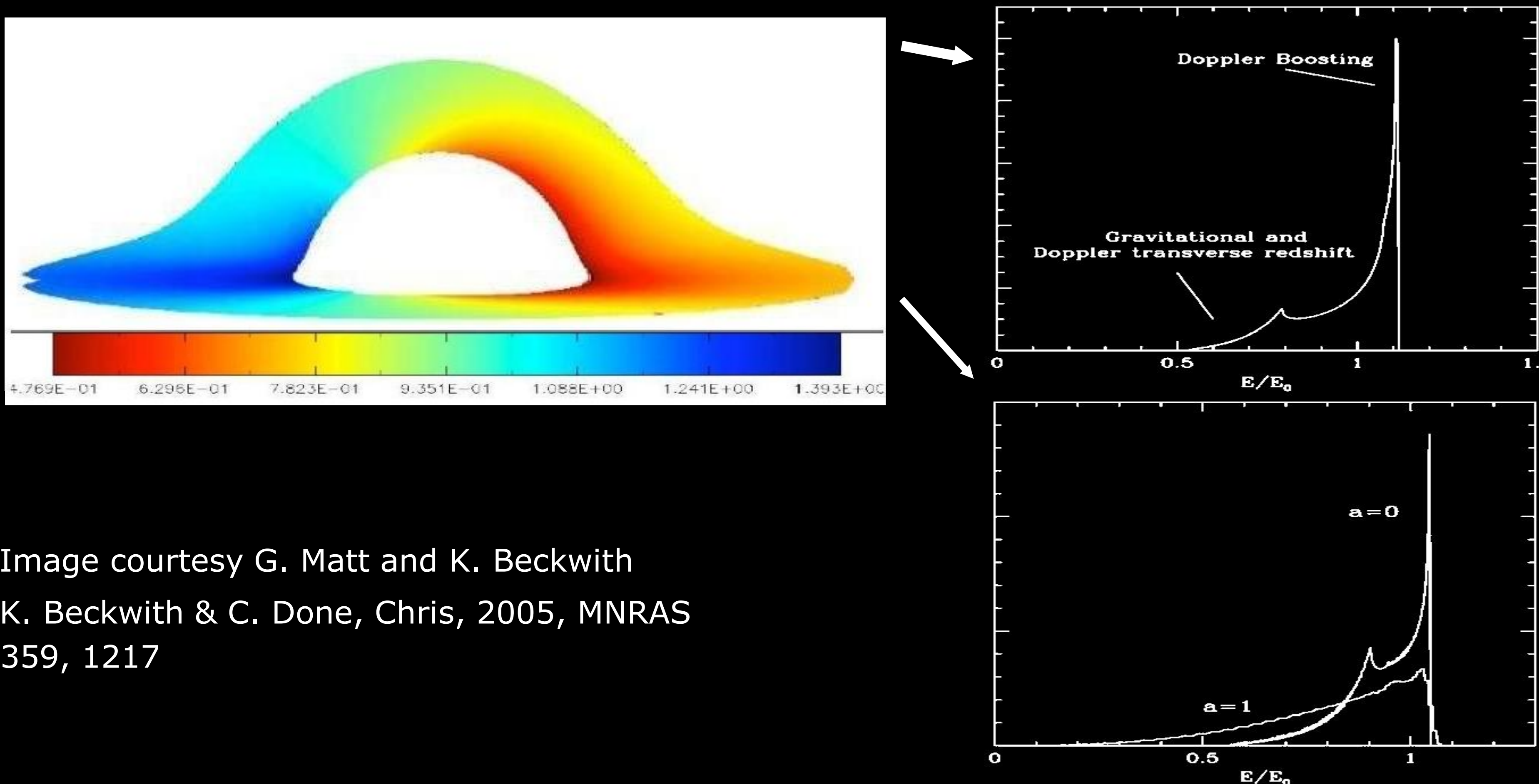

- Image courtesy G. Matt and K. Beckwith
- K. Beckwith & C. Done, Chris, 2005, MNRAS 359, 1217

XTE J1650-500 in its 2001 Outburst

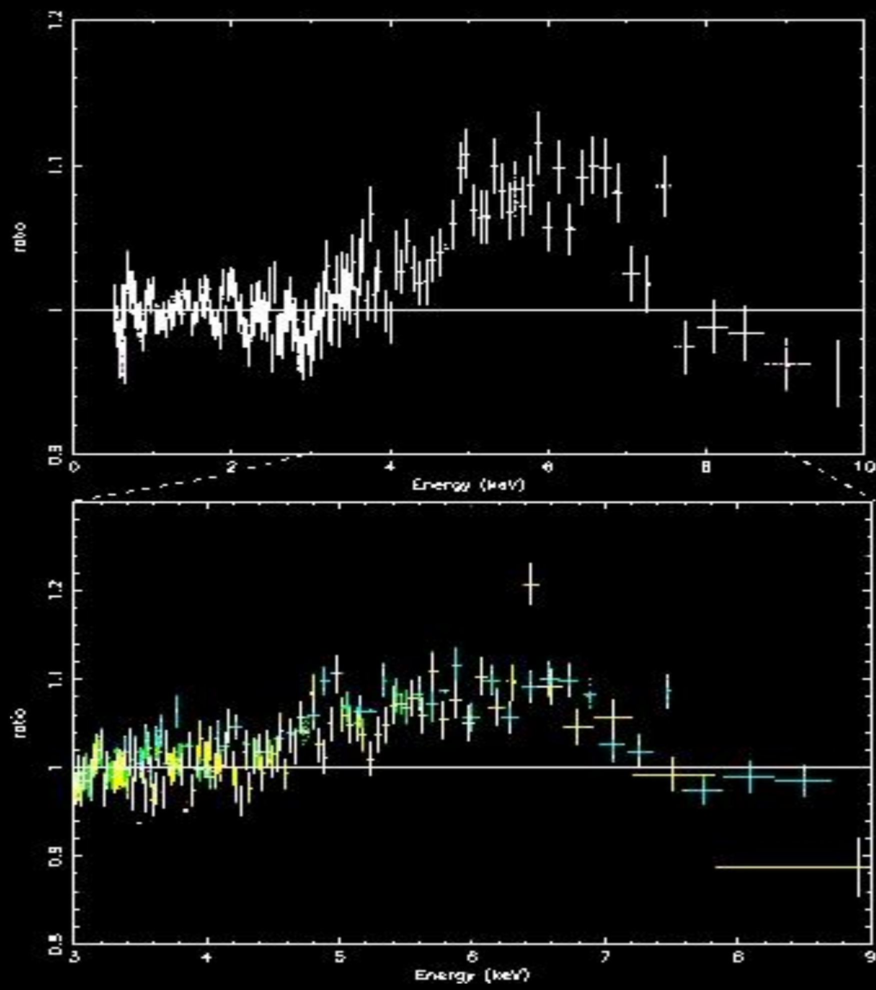

- Broad, skewed Fe Kα emission line suggests the primary in this system may be a Kerr black hole
- Steep disk emissivity profile that is hard to explain in terms of a standard accretion disk model

➔ May be explained by the extraction and dissipation of rotational energy from a black hole with nearly maximal angular momentum

J. M. Miller, et al. 2002, ApJ 570, L69

5 –15 solar masses

MCG-6-30-15: Extraction of Energy from the Spinning Black Hole

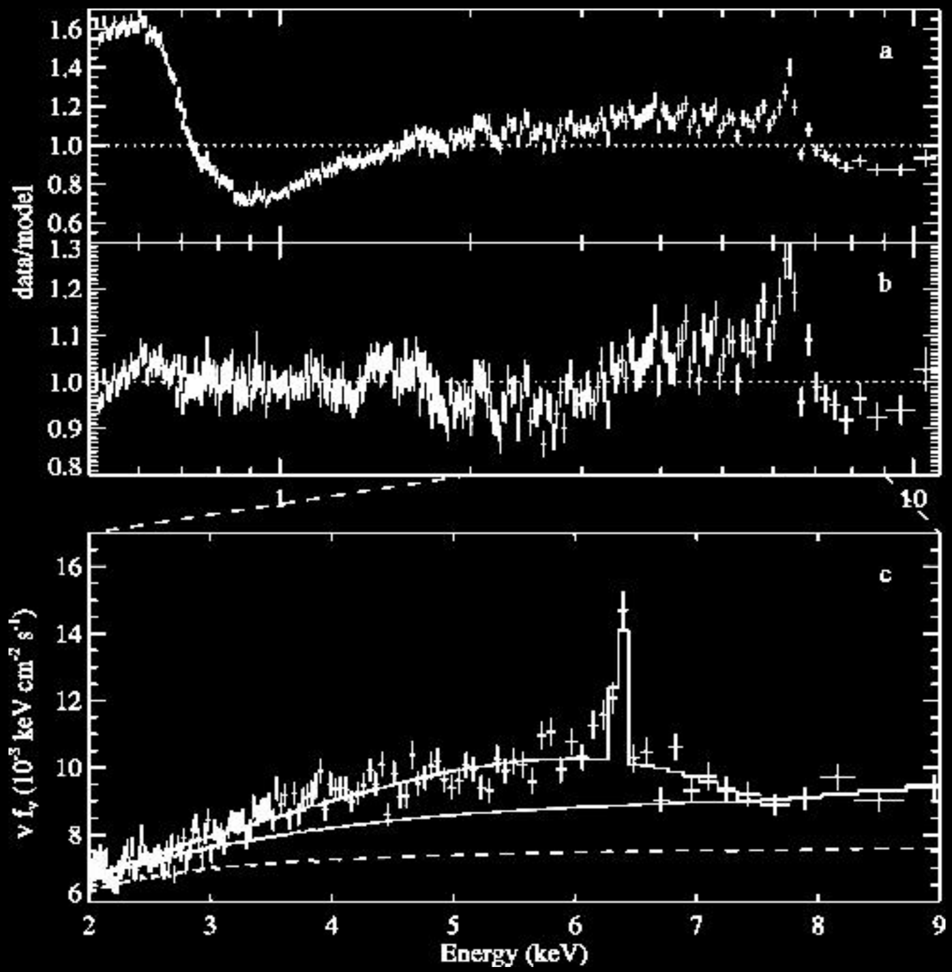

- `Deep minimum' state
- Difficult to understand in any pure accretion disc model

➔ Extraction and dissipation of rotational energy from a spinning black hole

J. Wilms et al., 2001, MNRAS 328, L27

10^6–10^8 solar masses

A rapidly spinning supermassive black hole at the centre of NGC1365

Simultaneous observation of NGC 1365 by XMM-Newton and NuSTAR:

➔ relativistic disk features through broadened Fe-line emission and an associated Compton scattering excess of 10-30 keV

➔ temporal and spectral analyses allows to disentangle continuum changes due to time-variable absorption from reflection, which arises from a region within 2.5 gravitational radii of the rapidly spinning black hole.

➔ Absorption-dominated models that do not include relativistic disk reflection can be ruled out both statistically and on physical grounds.

Risaliti G., et al., 2013, Nature 494

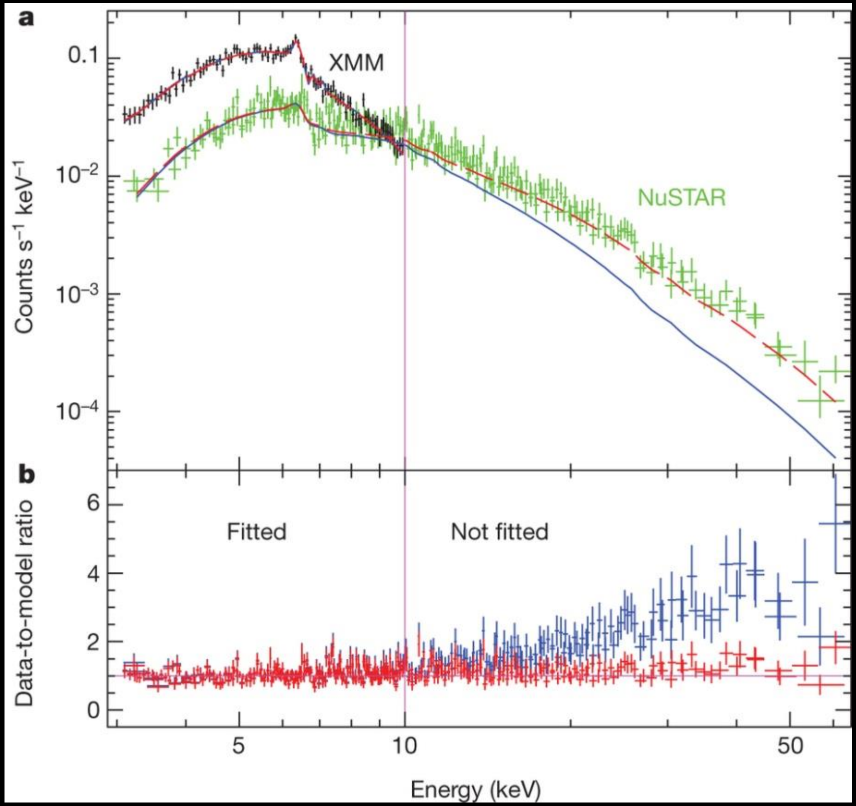

a: XMM-Newton and NuSTAR spectral data and models. The two models contain a relativistic reflection component plus variable partial covering (red), and a double partial covering (blue). Both models have been fitted to the data below 10 keV, and reproduce the lower-energy data well. However, the models strongly deviate at higher energies. b, Data-to-model ratio for the double partial covering (blue) and relativistic reflection plus variable absorber (red) models.

Determination of the angular momentum …

Outburst of the Galactic Black Hole GX 339-4

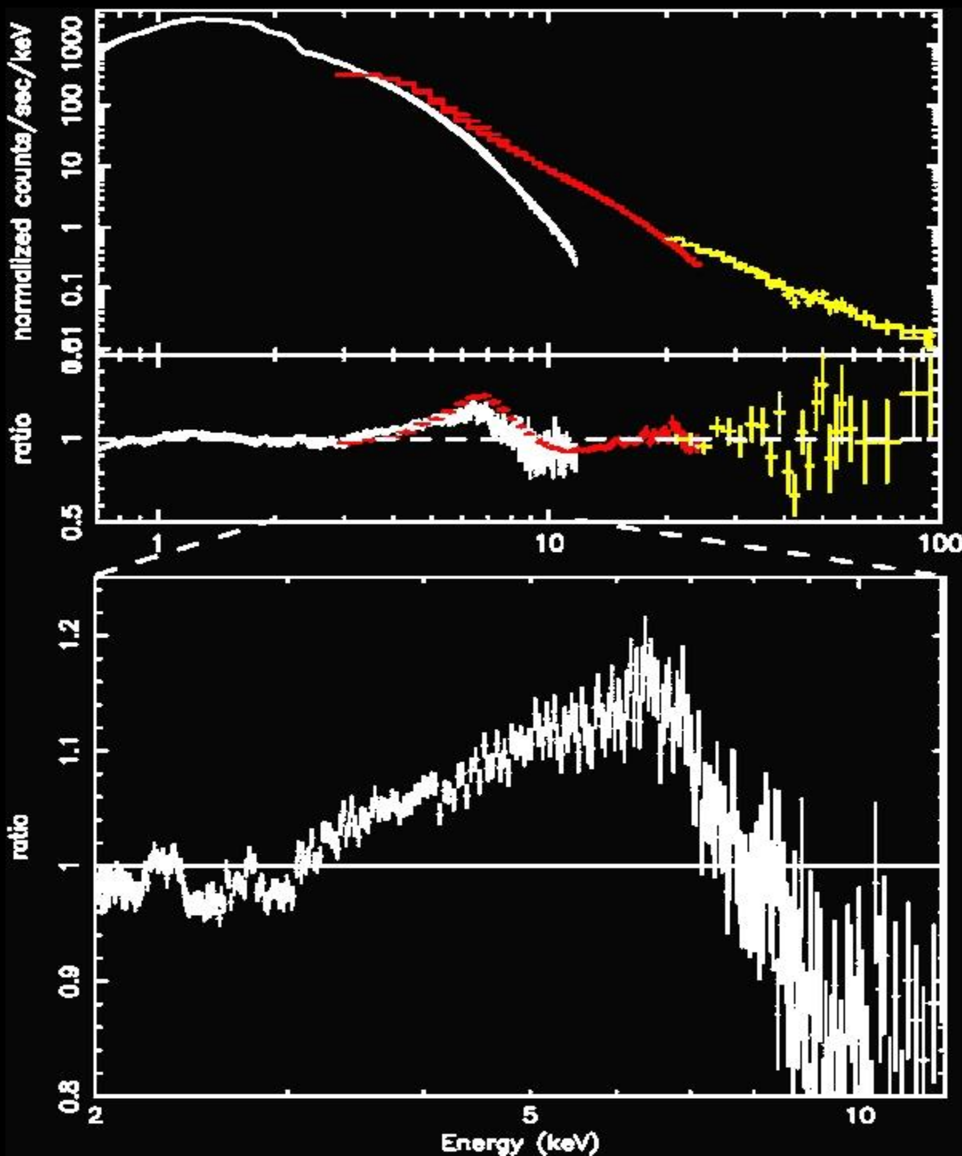

- Extremely skewed, relativistic Fe Kα emission line and ionized disk reflection spectrum
- Inner disk radius is not compatible with a Schwarzschild black hole

➔ Black hole with a>0.8-0.9 (where rg=GM/C^2 and a=cJ/GM^2)

J.M Miller et at., 2004, ApJ 606, L131

Broad line emission from iron K- and L shell transitions in the active galaxy 1H 0707-495

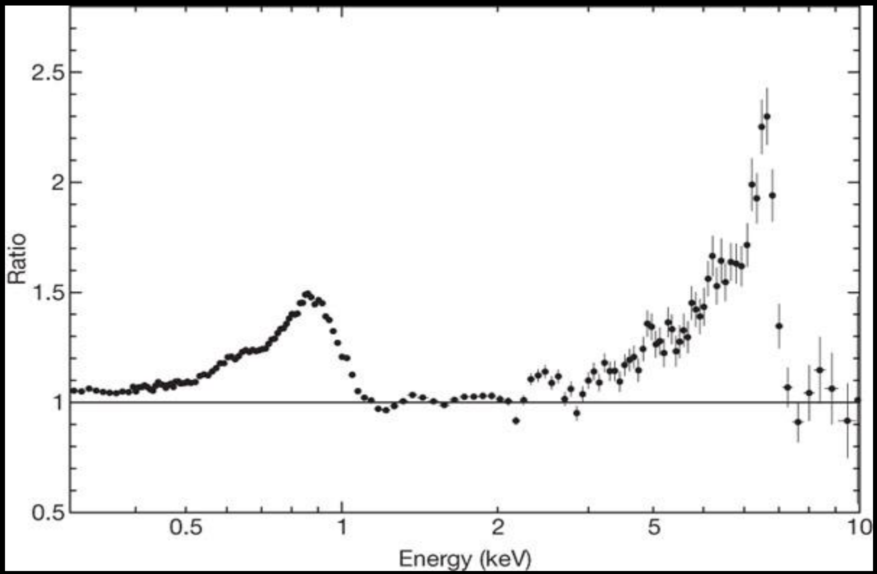

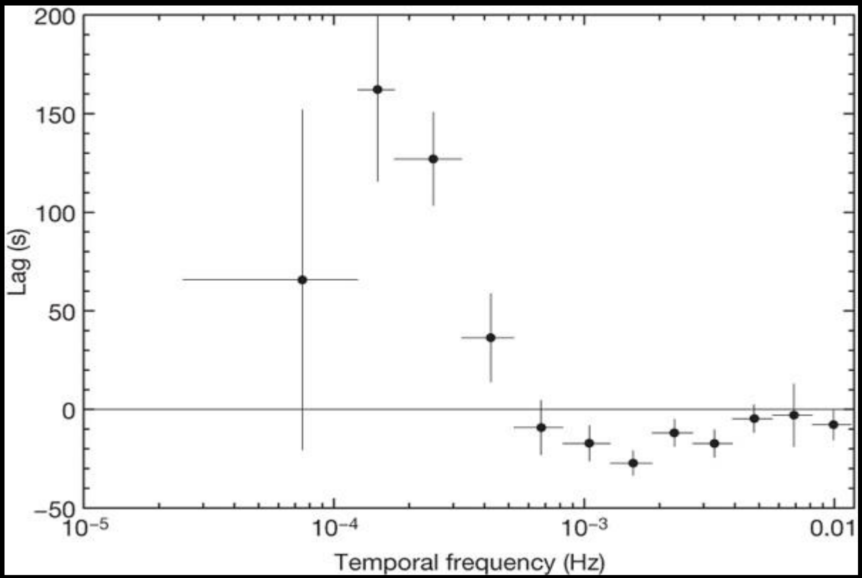

Broad Iron K & L emission lines :

- Line ratio (photons) 1:20
- Emitted between 1.3 and 400 r_g
- Emissivity index 4
- BH spin rate a > 0.98

➔ Frequency-dependent lags between the 1 - 4 kev band flux and the 0.1 – 1 keV band flux

- ➔ Negative lag for ν > 6 x 10^{-4} Hz
- ➔ Power law changes before refection

A.C. Fabian, 2009, Nature 459, 540

… 1H 0707-495 …

1H0707-495 in 2010: mildly relativistic ionized outflow

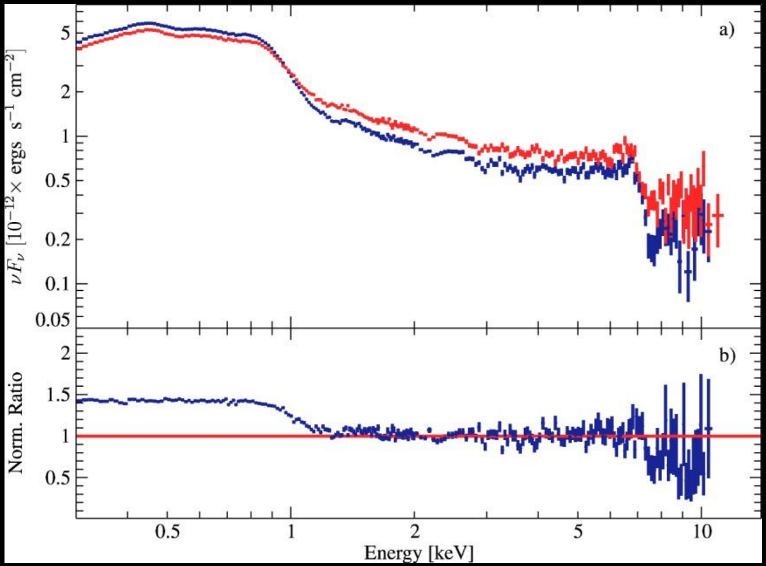

- Second 500 ks XMM-Newton & 120 ks Chandra observation of 1H0707-495 in 2010 September.

➔ Consistent with Fabian et al. (2009) and Zoghbi et al. (2010)

T. Dauser, et al., 2011arXiv1112.1796D

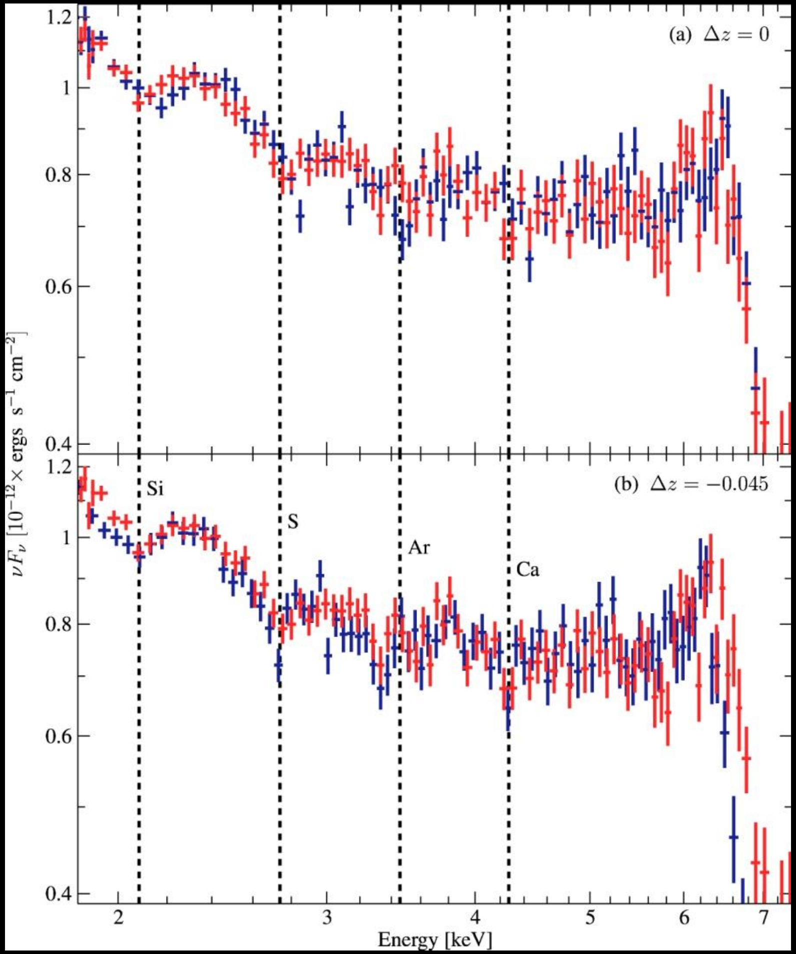

➔ spectrum is dominated by relativistically broadened reflection from an ionized accretion disc around a maximally rotating black hole

➔ Physical parameters of the black hole and accretion disc (i.e., spin and inclination) are consistent between both observations.

➔ Absorption in a mildly relativistic, highly ionized outflow which changed velocity from around 0.11c to 0.17c between 2008 January and 2010 September

1H0707-495 in low state: An X-ray source within a gravitational radius of the event horizon

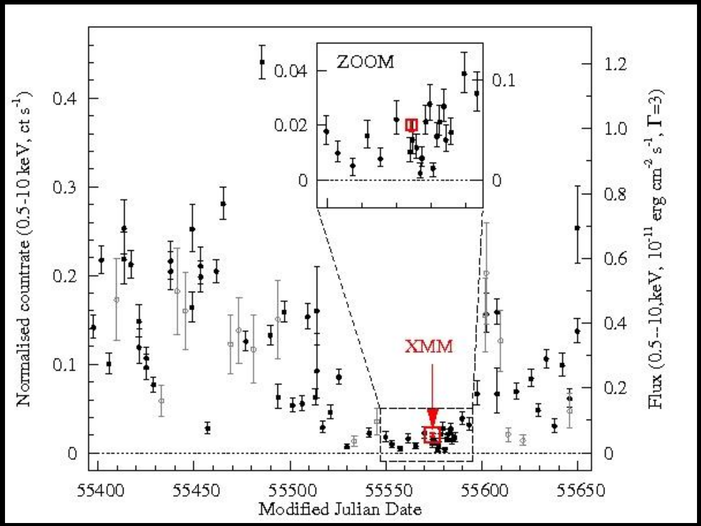

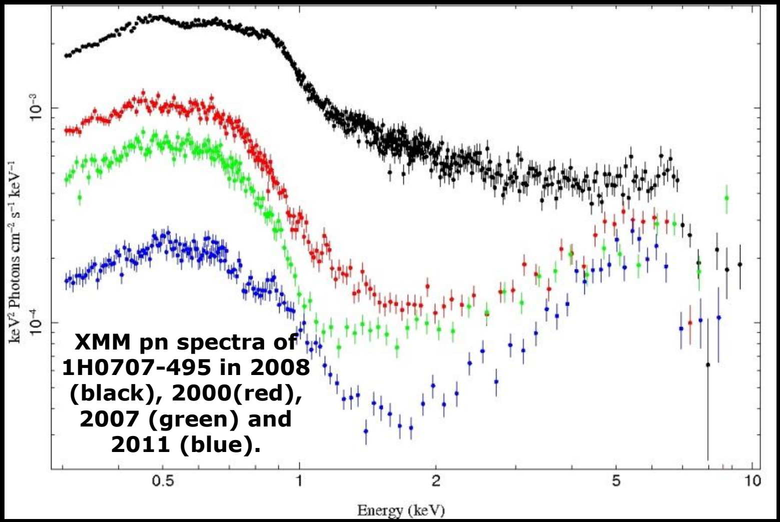

Fabian, A. C. et al., 2012, MNRAS 416, 116

- The Narrow Line Seyfert 1 Galaxy 1H0707-495 was in a low state from 12/2010 to 2/2011 February, discovered by monitoring of Swift
- 100 ks XMM-Newton observation of the low state: flux has dropped by a factor of 10 in the soft band, and a factor of 2 at 5 keV, compared with a long observation in 2008
- The spectrum is well fit by a relativistically-blurred reflection spectrum

➔ The irradiating source must lie within 1 gravitational radius of the event horizon of the black hole, which spins rapidly.

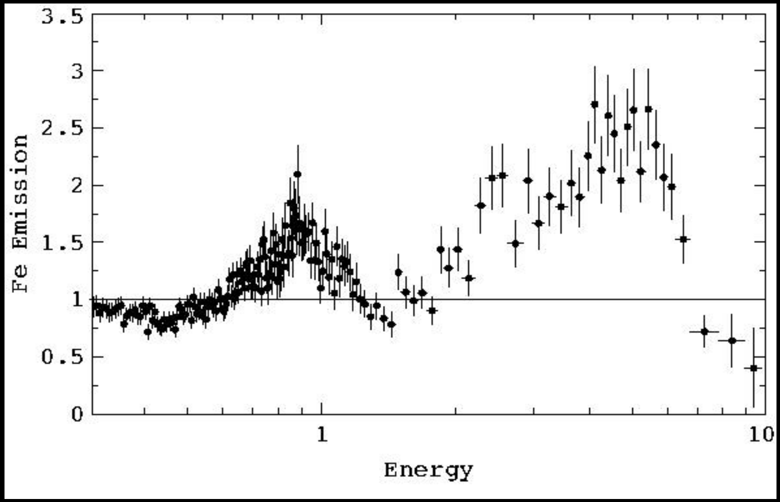

1H0707-495 in low state: An X-ray source within a gravitational radius of the event horizon

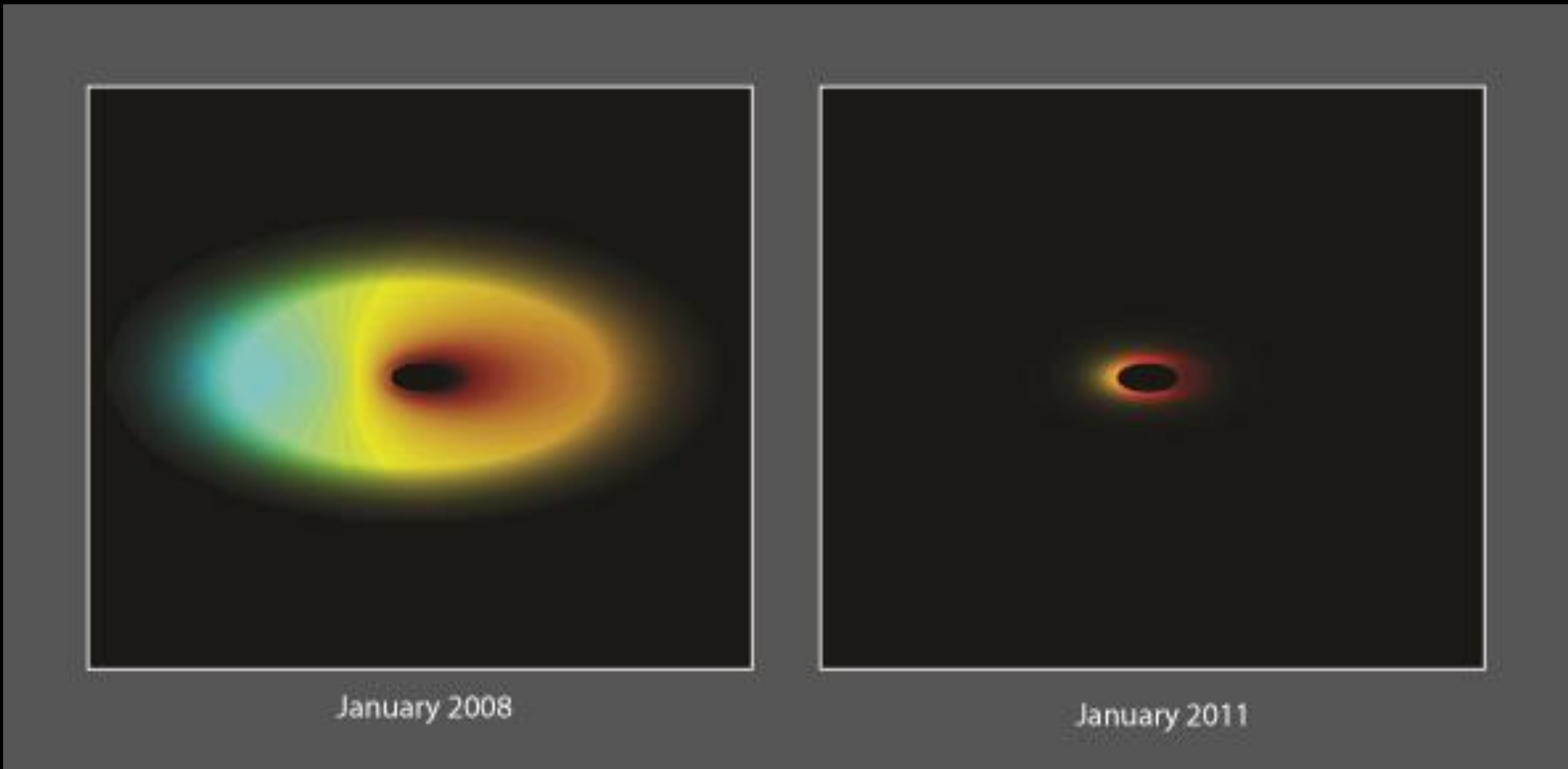

Courtesy Dan Wilkins; A.C. Fabian et al., 2012, MNRAS 419, 116

Reflection from the strong gravity regime in a quasar at redshift z = 0.658

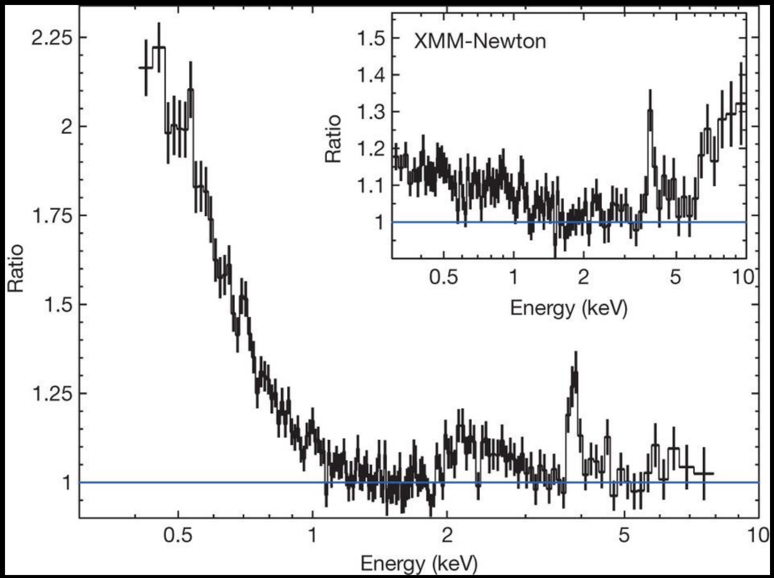

R. C. Reis, et al., 2014, Nature 507, 207

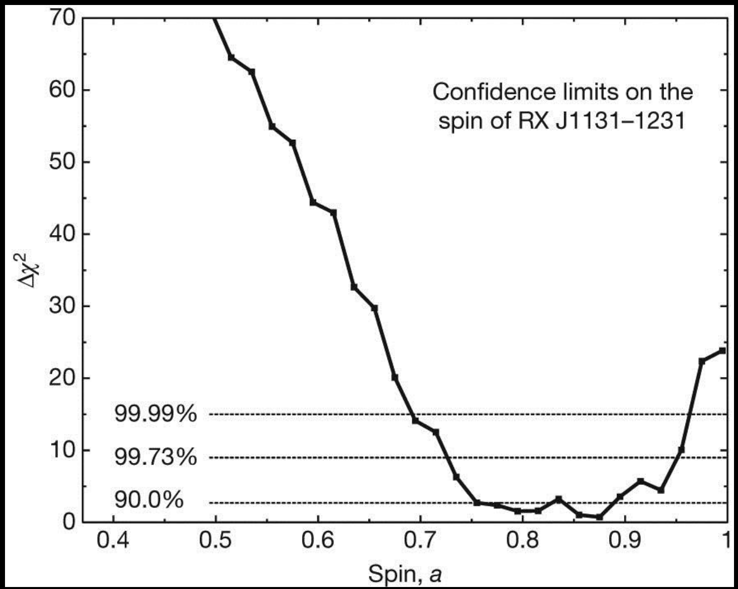

➔ The emission originates within three gravitational radii from the black hole, implying a spin parameter of $a = 0.87^{+0.08}_{-0.15}$ at the 3σ confidence level and a > 0.66 at the 5σ level.

➔ The high spin is indicative of growth by coherent accretion for this black hole, and suggests that black-hole growth at 0.5 <= z <= 1 occurs principally by coherent rather than chaotic accretion episodes.

… variability near to the event horizon…

Orbital Motion Close to the Central Black Hole of Mrk 766

- Energy-time plane of EPIC pn data in the 4-8 keV band
- Fe Kα emission shows a variation of photon energy with time con-sistent with sinusoidal variation

➔ Orbit has a period ~165 ks and a line-of-sight velocity ~13,500 km/s

- $4.9 \times 10^5 < M_{BH} < 4.5 \times 10^7$

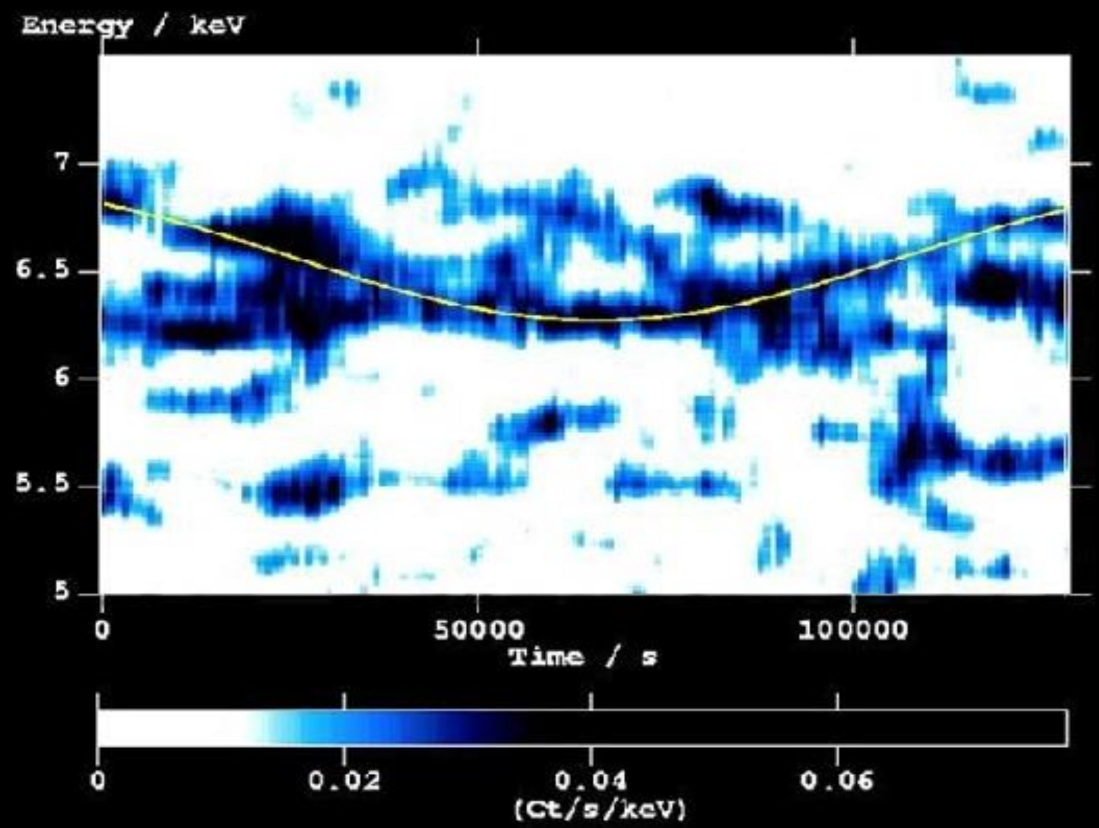

T. J. Turner, et al., 2006, A&A 445, 59

Flux and Energy Modulation of Iron Emission in NGC 3516

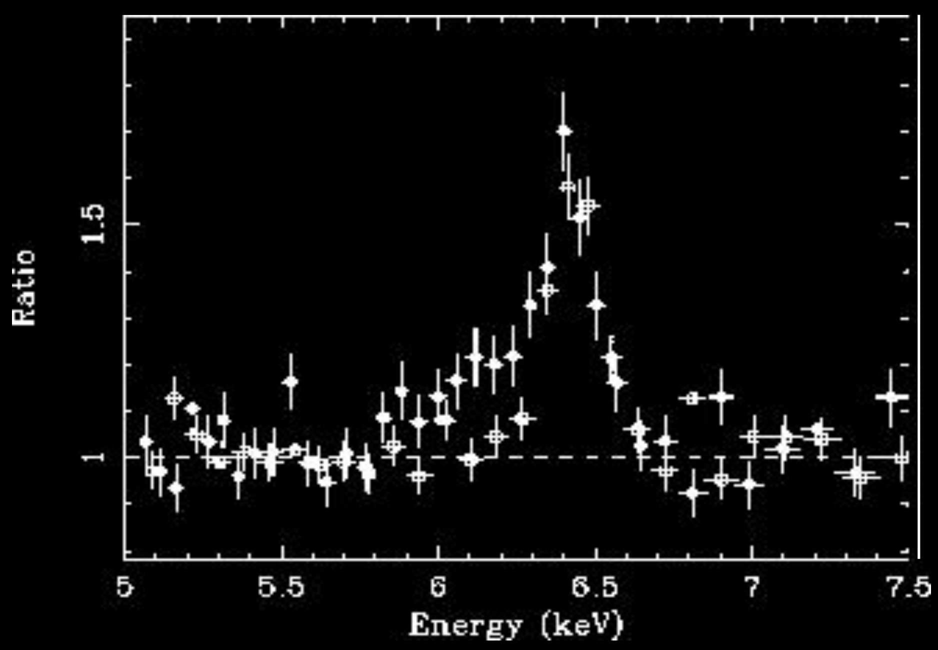

K. Iwasawa, G. Miniutti & A.C. Fabian, 2004, MNRAS 355, 1073

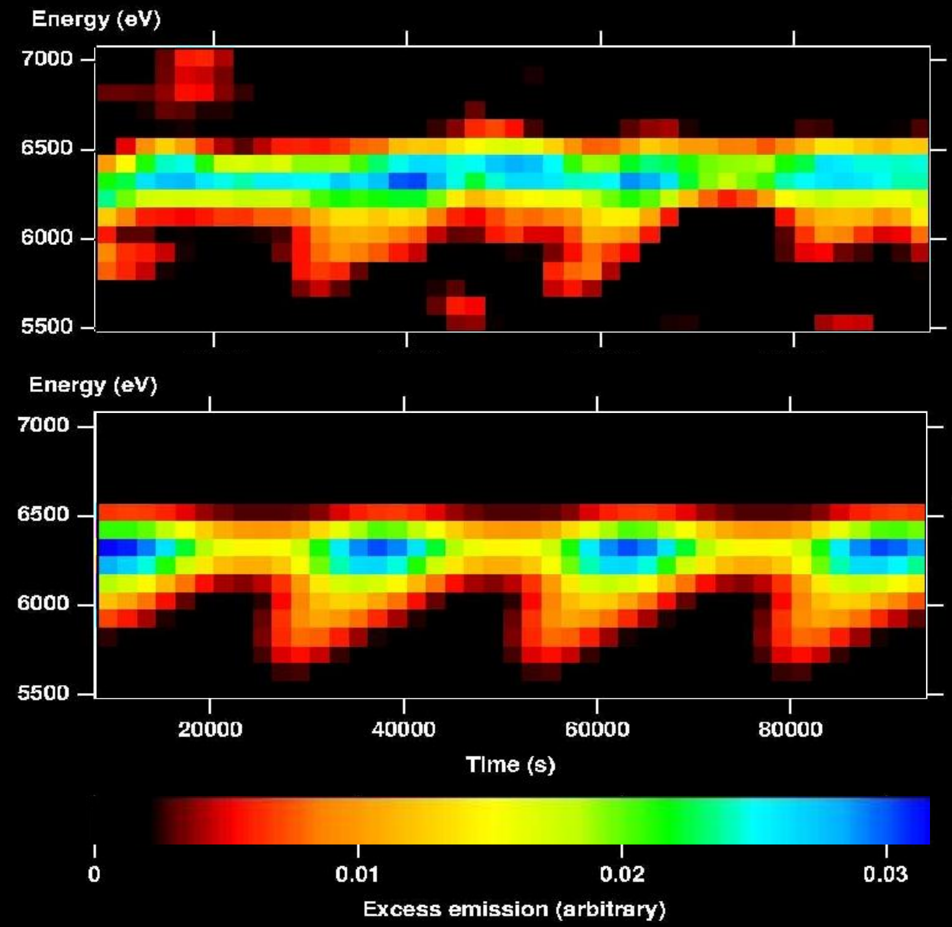

- "co-rotating" flare at a (3.5-8) r_{Sch}
- mass of the BH: (1-5) × $10^7 M_o$

First QPO from an AGN

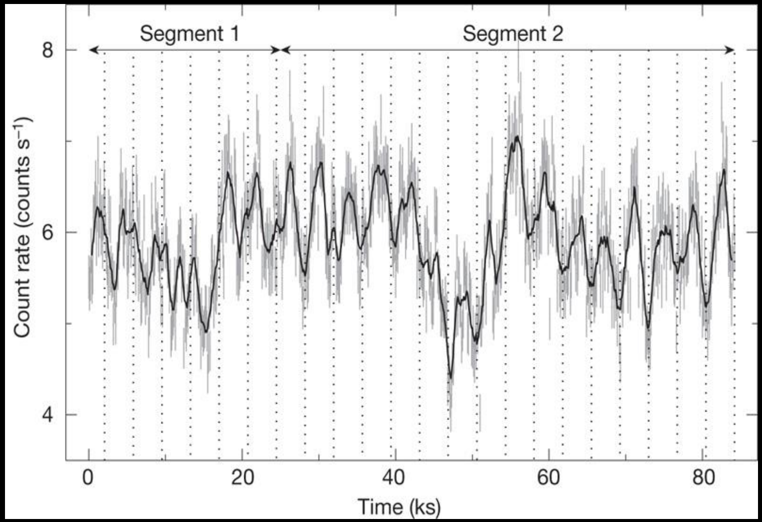

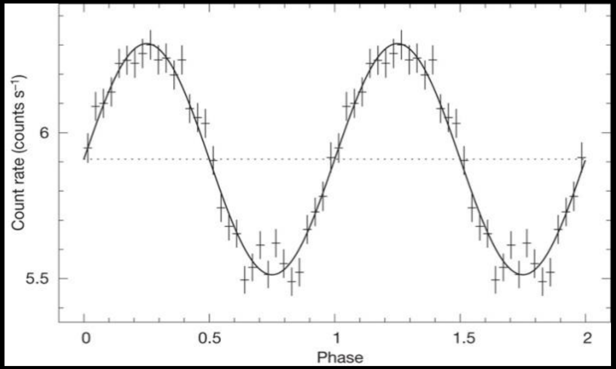

Gierlinski et al., 2008, Nature 455, 369

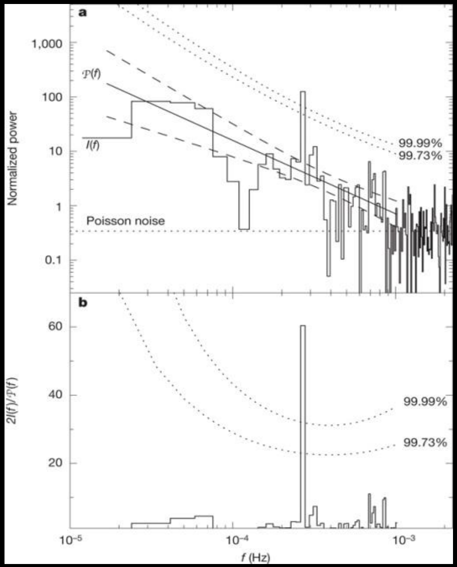

- Since 20 years QPO in X-ray binaries, but never found for AGNs (13y)
- RE J1034+396 nearby (z=0.043) narrow-line Seyfert 1
- Black hole mass: 6.3 x 10^5 to 3.6 x 10^7 M_{sun}

➔ XMM-Newton detection of a ~ 1 hour quasi periodic oscillation (QPO)

➔ Provides fundamental length-scale of SMBH system

… feedback to the theory …

X-Ray Flare of the Galactic Center BH

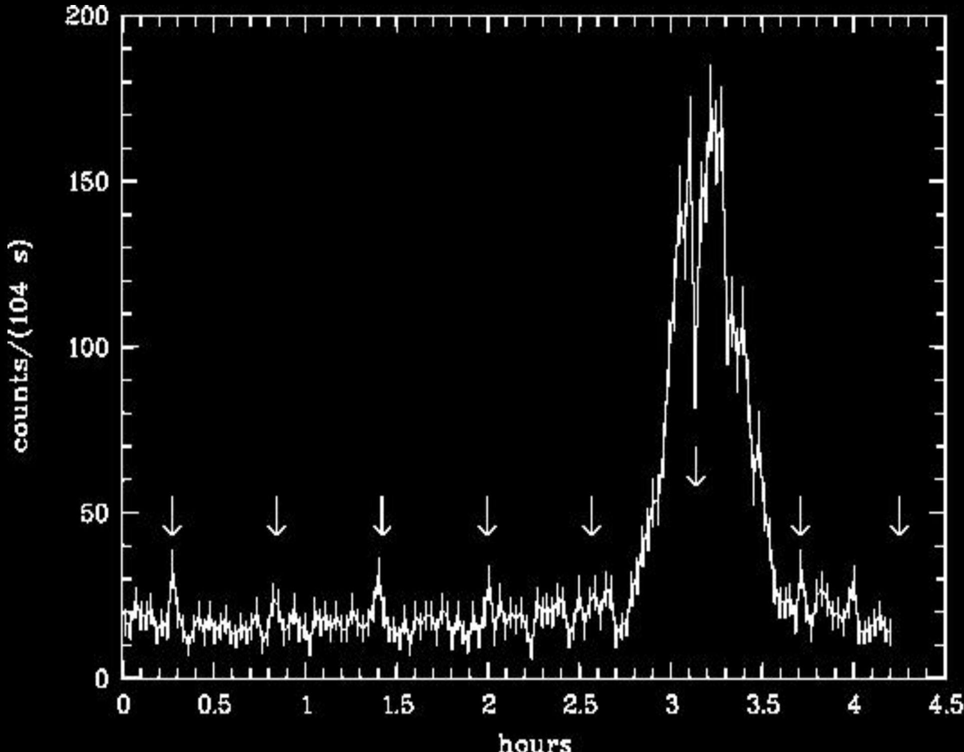

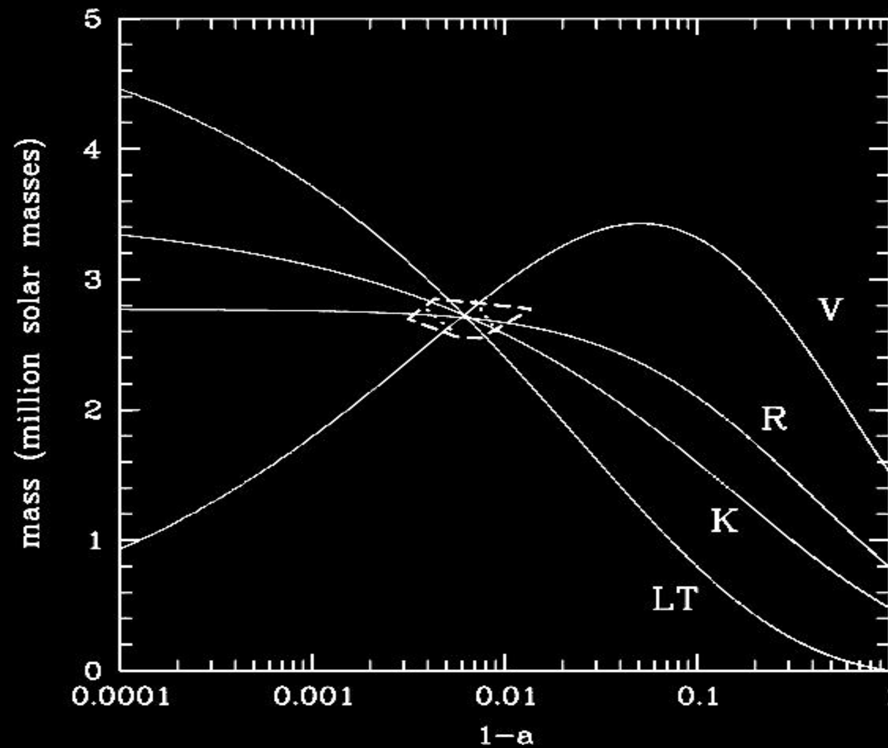

B. Aschenbach et al., 2004, A&A 417, 71

-Power density spectrum peaks at periods of 100s, 219s, 700s, 1150s and 2250s

Microquasars / Galactic Center BH

- GRO J1655-40, XTE J1550-564 and GRS 1915+105 show twin high frequency quasi-periodic oscillations with a ratio of 3:2 and/or 3:1
- resonance between vertical and radial epicyclic oscillations and Kepler orbits

➔ New topological structure

➔ Galactic Center BH:

$a = 0.99616$

$M = (3.28 \pm 0.13)\ 10^6 M_O$

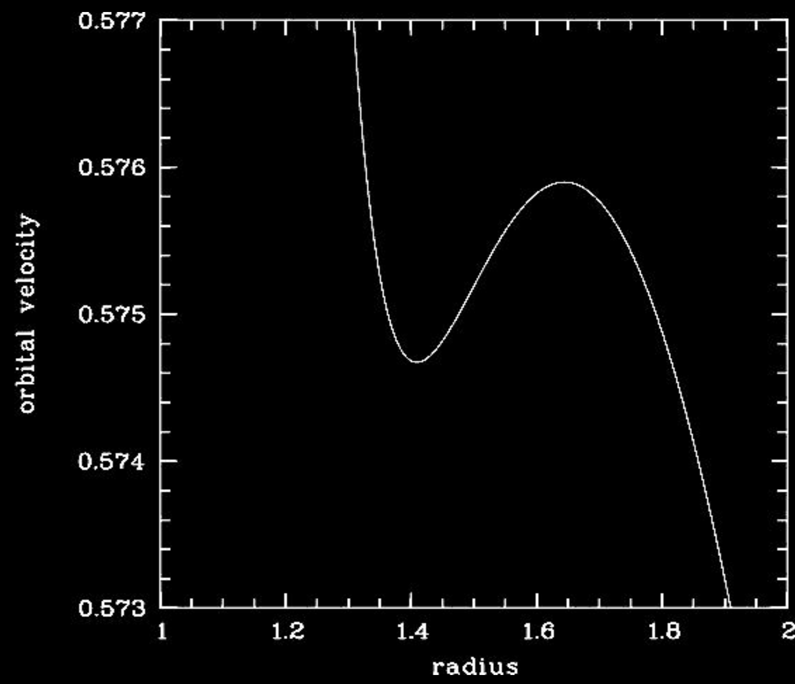

B. Aschenbach, 2004, A&A 425, 1075

PHYSICAL REVIEW D **71**, 024037 (2005)

Aschenbach effect: Unexpected topology changes in the motion of particles and fluids orbiting rapidly rotating Kerr black holes

Zdeněk Stuchlík,[1,2,*] Petr Slaný,[1,2,†] Gabriel Török,[1,2,‡] and Marek A. Abramowicz[1,2,3,§]

[1]*Institute of Physics, Silesian University at Opava, Bezručovo nám. 13, CZ-746 01 Opava, Czech Republic*
[2]*NORDITA, Blegdamsvej 17, DK-2100 Copenhagen, Denmark*
[3]*Theoretical Physics, Göteborg & Chalmers Universities, S-412 96 Göteborg, Sweden*
(Received 12 November 2004; published 28 January 2005)

.. Tidal disruption events

Huge Drop in the X-Ray Luminosity of the Nonactive Galaxy RX J1242.6-1119A

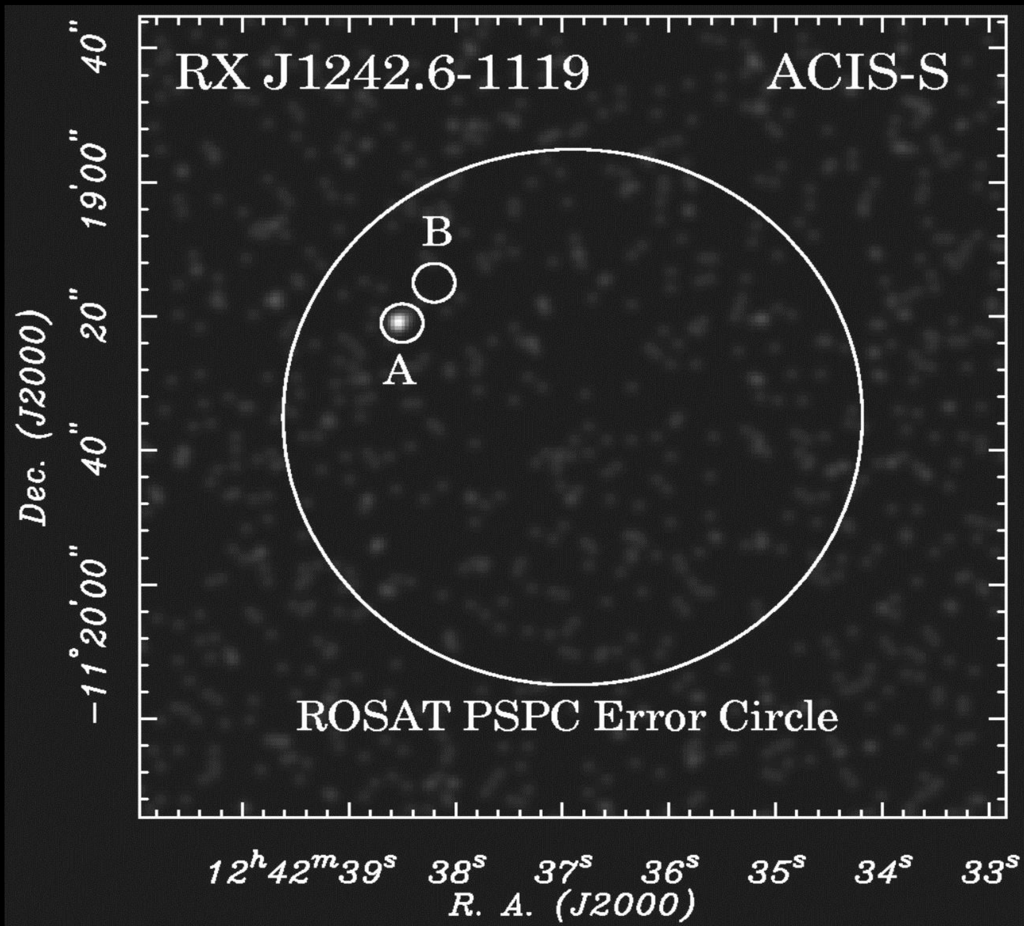

- ROSAT, Chandra and XMM-Newton
- ~200 drop in X-ray luminosity

➔ (Partial or complete) tidal disruption of stars captured by the black holes

S. Komossa et al., 2004, ApJ 603. L17

Tidal Disruption: Swift J164449.3+573451

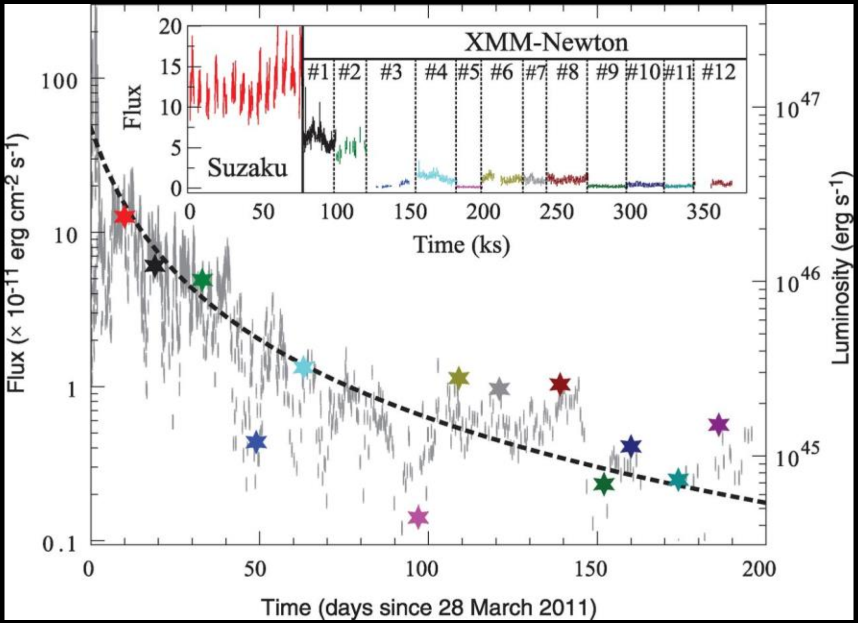

- tidal disruption of a star by a dormant black hole
- bright X-ray flares
- galaxy at redshift z = 0.3534

➔ ~200-second x-ray quasi-periodicity

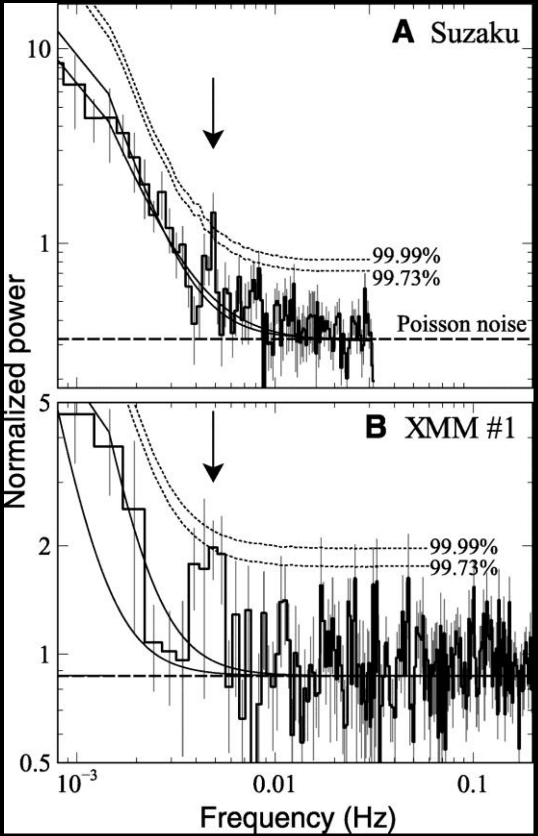

R.C. Reis et al., 2012, Science, 337, 949

Flows of X-ray gas reveal the disruption of a star by a massive black hole

- XMM-Newton observation of the tidal disruption event ASASSN-14li

- detection of blue-shifted absorption lines of highly ionized atoms

- variability indicates that the gas is close to the black hole

- narrow line widths indicate a low volume filling factor

- outflow speeds are below the escape speed from the radius set by variability

➔ rotating wind from the inner region of a nascent accretion disk,

or with a filament of disrupted stellar gas near to the apocenter of an elliptical orbit

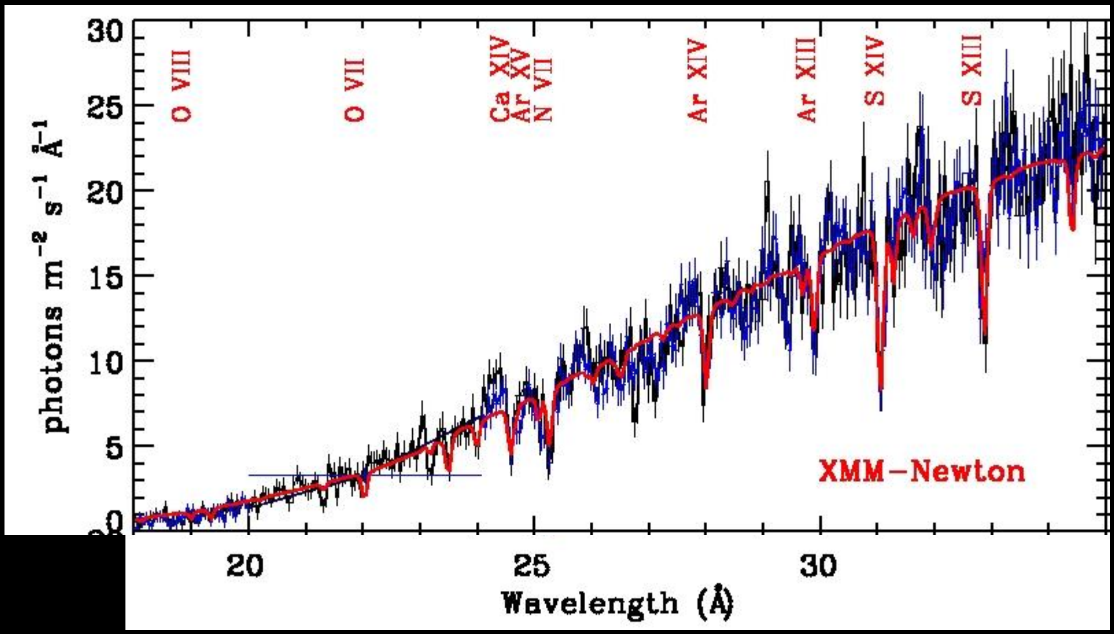

The high-resolution X-ray spectra of ASASSN-14li reveal blue-shifted absorption lines. XMM-Newton spectra from the RGS1 and RGS2 units are shown in black and blue.

J.M. Miller et al., 2015, Nature 526, 542

.. winds and outflows ..

Compact, Conical, Accretion-Disk Warm Absorber Of The Seyfert 1 Galaxy NGC 4051

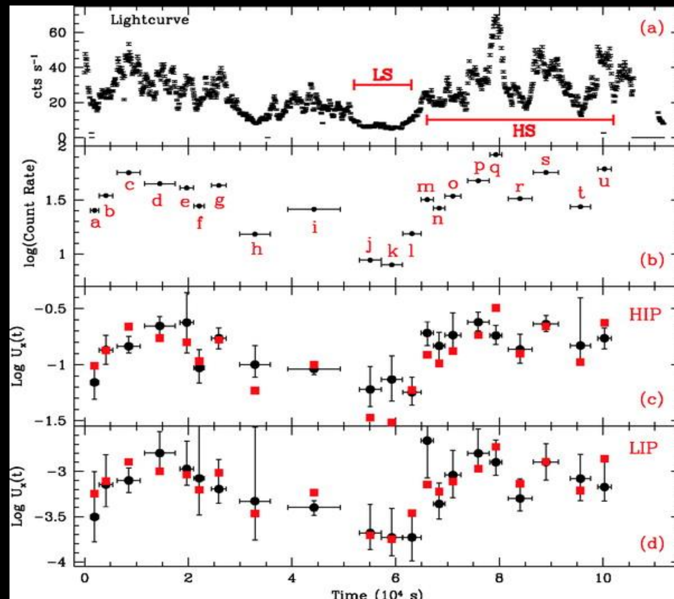

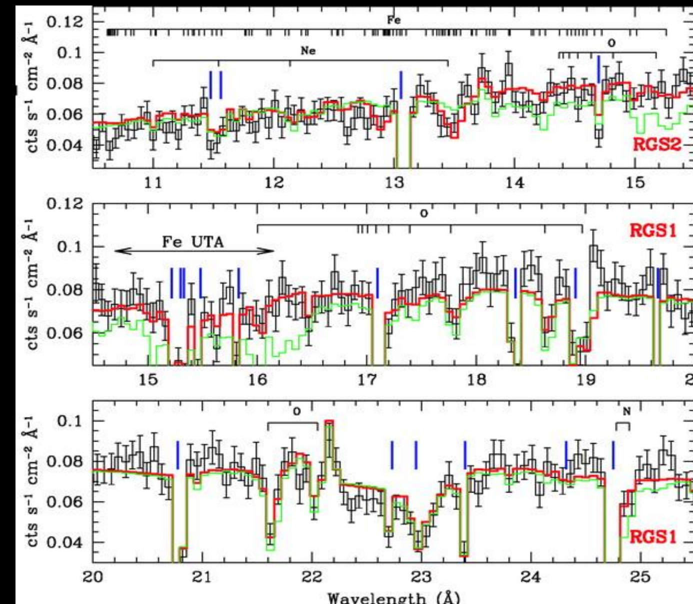

- Absorber consists of two different ionization components, with a difference of ~100 in ionization parameter and ~5 in column density
- Distances 0.5-1.0 lt-days (2200RS-4400RS) and <3.5 lt-days (<15,800 RS) from the continuum source

➔ Suggests strongly accretion-disk origin for the warm absorber wind

➔ Mass outflow rate from wind is 2%-5% of the mass accretion rate

Krongold et al., 2007, ApJ 659, 1022

Ultra-fast Outflows in Radio-quiet Active Galactic Nuclei

- ➔ Location is in the interval ~0.0003-0.03pc ($\sim 10^2$-10^4 r_s) from the central black hole
- ➔ Outflow rates: ~0.01-1 Mo y^{-1} / 5-10% of the accretion rates
- ➔ Mechanical power ~42.6-44.6 erg s^{-1}
- ➔ UFOs provide a significant contribution to the AGN cosmological feedback, in agreement with theoretical expectations

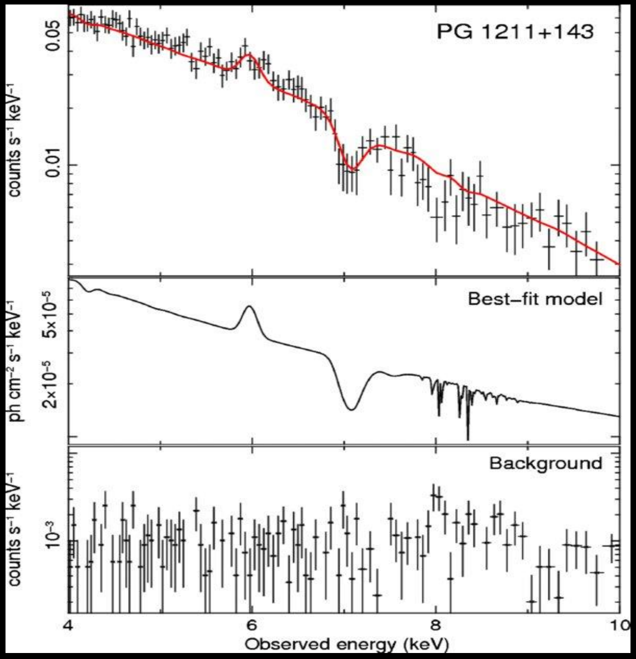

- Ultra-fast outflows (UFOs) are detected through blueshifted Fe XXV/XXVI K-shell transitions.
- 42 local radio-quiet AGNs observed with XMM-Newton.

- ➔ >35% are showing UFOs
- ➔ v ~ 0.03c -0.3c, mean value of ~0.14c
- ➔ Ionization parameter is very high: log $\xi \sim 3$-6 erg s^{-1} cm
- ➔ Column densities are $N_H \sim 10^{22}$-10^{24} cm^{-2}

F. Tombesi et al., 2012, MNRAS 422, L1

F. Tombesi, et al., 2011, ApJ 742, 44

F. Tombesi, et al., 2010, A&A 521, 57

Black hole feedback in the luminous quasar PDS 456

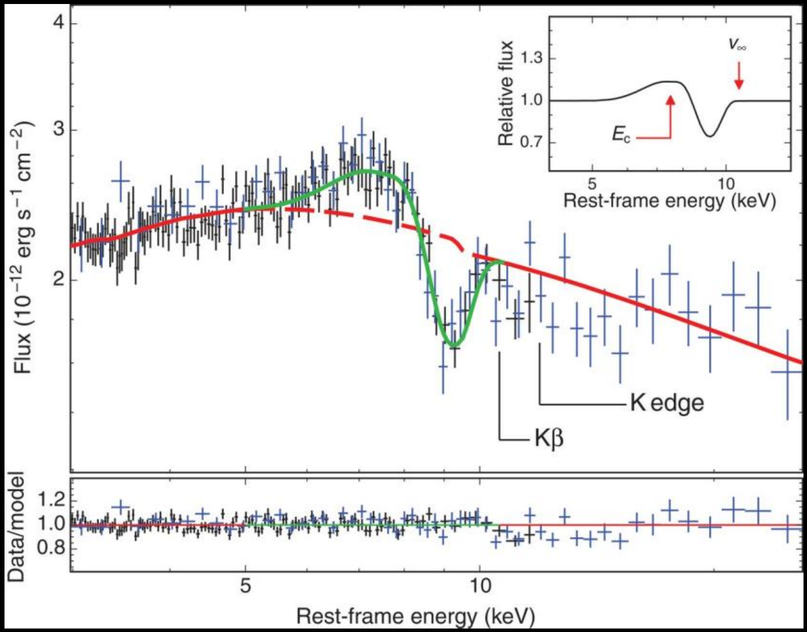

XMM-Newton pn data are shown in black and NuSTAR data are shown in blue. The green curve shows a model where the emission and absorption residuals characterizing the Fe-K band are described through a self-consistent P-Cygni profile from a spherically symmetric outflow.

- XMM-Newton and NuSTAR simultaneously observed PDS 456 on four occasions in 2013

- The emission and absorption residuals of the Fe-K band are described through a self-consistent P-Cygni profile

➔ Nearly spherical symmetric outflow of highly ionized gas

➔ This wind is expelled at relativistic speeds from the inner accretion disk

➔ The outflow's kinetic power >10^{46} ergs/s

➔ Enough to provide the feedback required by models of black hole and host galaxy coevolution.

E. Nardini, et al., 2015, Science 347, 860

.. AGN evolution ..

An Optically Obscured AGN in a Low Mass, Irregular Dwarf Galaxy

The distribution of supermassive black holes (SMBHs) in low-mass galaxies can provide important constraints on SMBH seed formation theories.

Using WISE data hundreds of dwarf galaxies were detected that display signatures of very hot dust highly suggestive of accretion onto massive BH

→ XMM-Newton follow-up observation of the irregular dwarf galaxy J132932.41+323417.0 reveals a hard, unresolved X-ray source with a luminosity $L_{2\text{-}10\ keV} = 2.4 \times 10^{40}$ erg/s, over two orders of magnitude greater than that expected from star formation, strongly suggestive of the presence of an accreting massive black hole.

➔ With a mass of $2.0 \times 10^{8}\ M_{\odot}$, this galaxy is similar in mass to the Small Magellanic Cloud, and is one of the lowest mass galaxies with evidence for a massive nuclear BH.

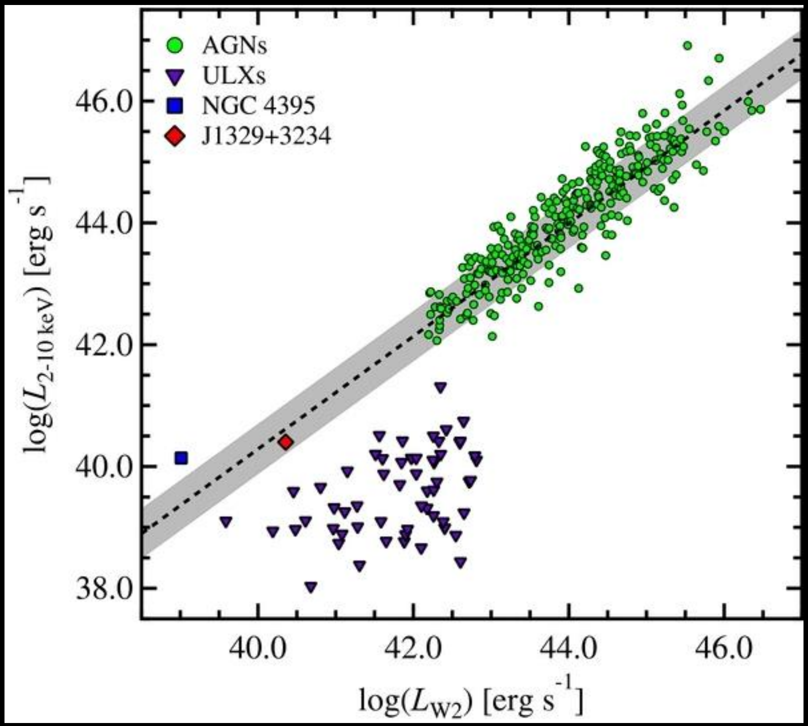

Observed 2–10 keV luminosity vs. the WISE infrared luminosity for a sample of AGNs, ULXs, and J1329+3234.

N. J. Secrest, et al., 2015, ApJ 798, 38

Luminosity-dependent evolution of soft X-ray selected AGN

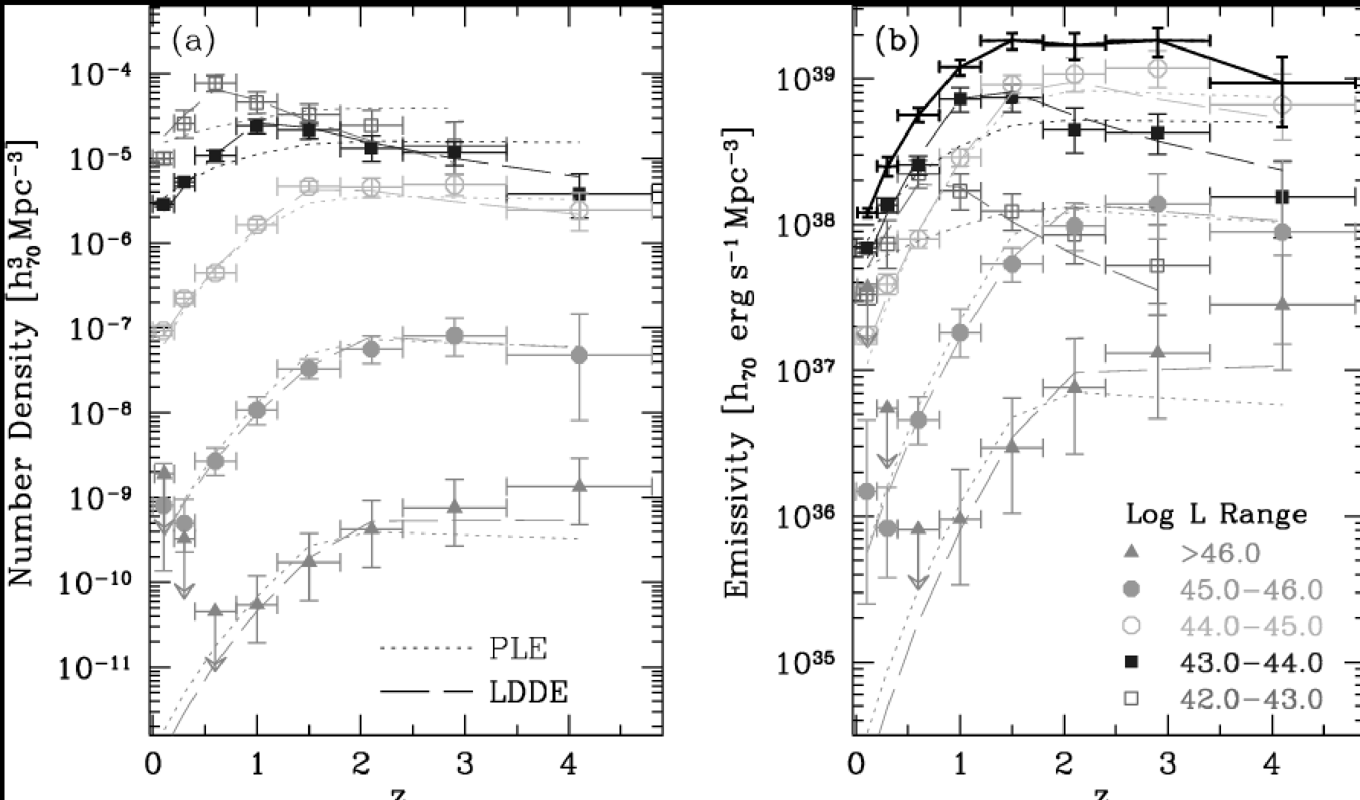

G. Hasinger, T. Miyaji & M. Schmidt, M., 2005, A&A 441, 417

- total of ~1000 AGN from a variety of ROSAT, XMM-Newton and Chandra surveys

➔ First time reliable space densities for low-luminosity (Seyfert-type) X-ray sources at cosmological redshifts.

➔ The evolutionary behaviour of AGN shows a strong dependence on X-ray luminosity: while the space density of high-luminosity AGN reaches a peak around z~2, the space density of low-luminosity AGNs peaks at redshifts below z=1. This confirms previous ROSAT findings of a luminosity-dependent density evolution.

X-ray observation of ULAS J1120+0641, the most distant quasar at z = 7.08

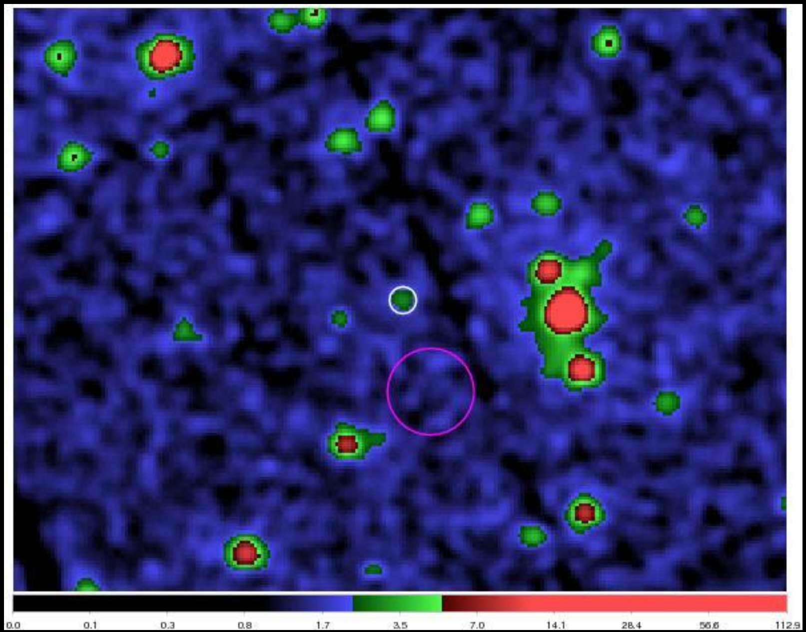

A. Moretti, et al., 2014, A&A 563, A46

and

M. J. Page, et al., 2014, MNRAS 440, L91

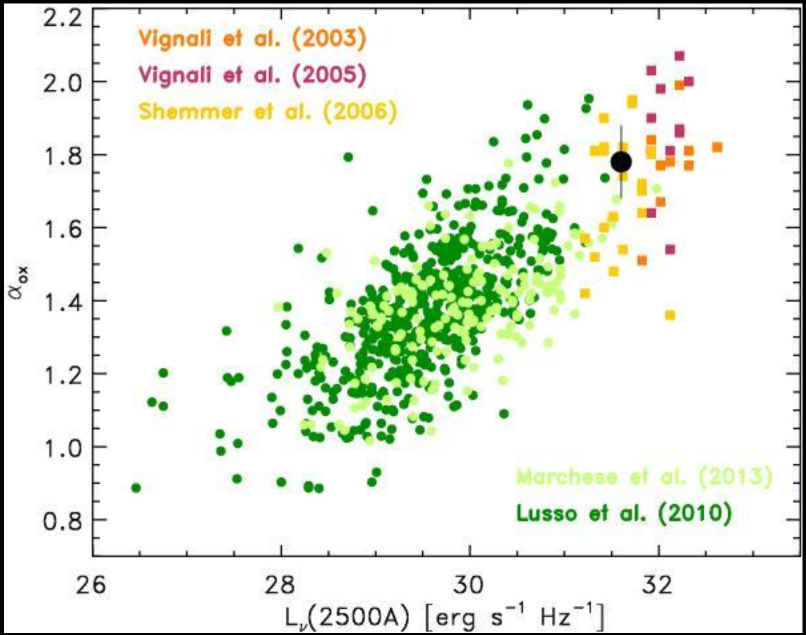

- ULAS1120+064 is the highest redshift quasar detected so far at z = 7.085
- It has been observed for 340 ks with XMM-Newton
- The 2-80 keV power-law spectrum shows photon index of 2.0 ± 0.3, a luminosity of $6.7 \pm 0.3 \times 10^{44}$ erg s^{-1} (2-10 keV), and an α_{OX} of 1.8 ± 0.1

➔ Agreement with the α_{OX} - luminosity correlation of low redshift quasars

➔ ULAS 1120+0641 is indistinguishable from the population of optically bright quasar at lowredshift

.. quasars as cosmological test ..

Iron Abundances: APM08279+5255

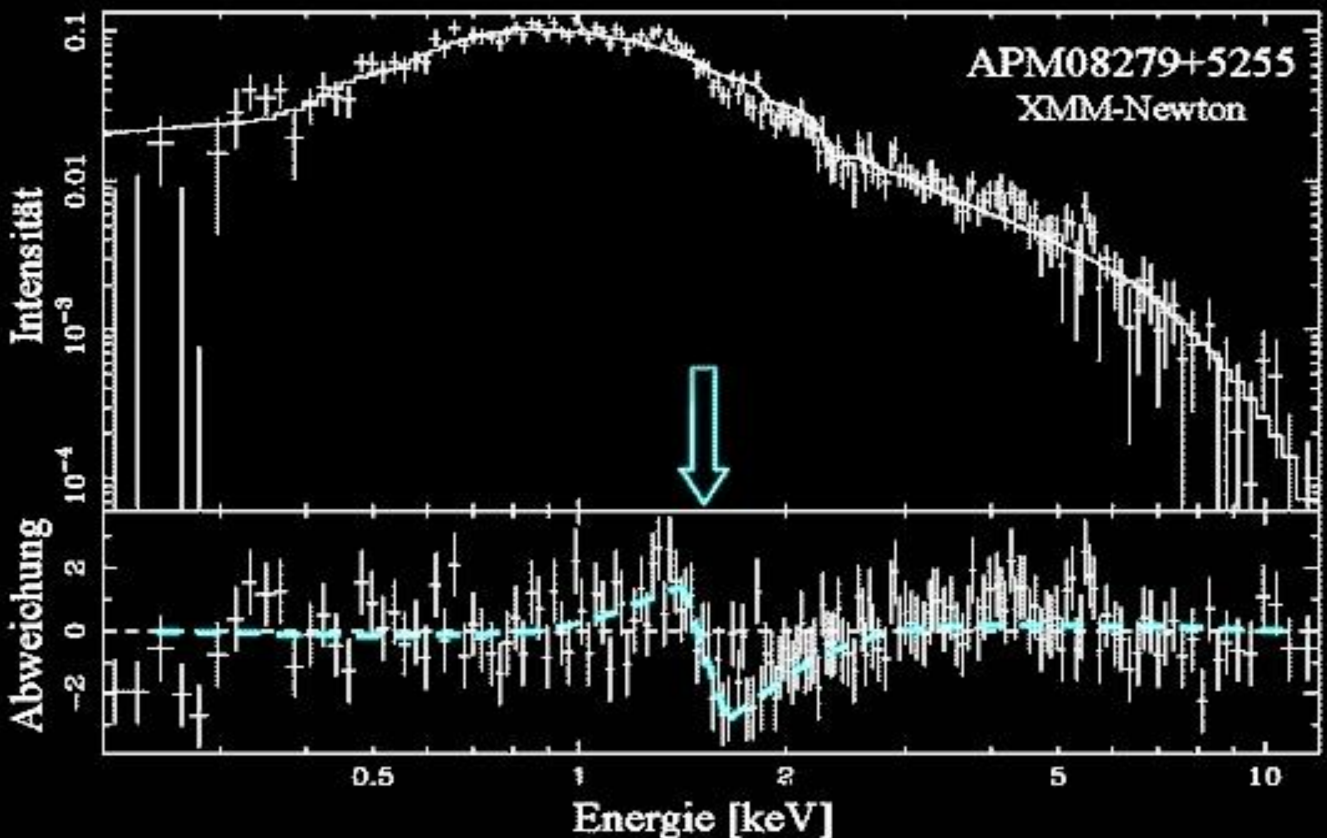

- Ionized Fe Kα edge in the z=3.91 broad absorption line quasar APM 08279 +5255

➔ Constraints on the age of the universe

G. Hasinger et al., 2002, ApJ 573, 77

A Hubble Diagram for Quasars

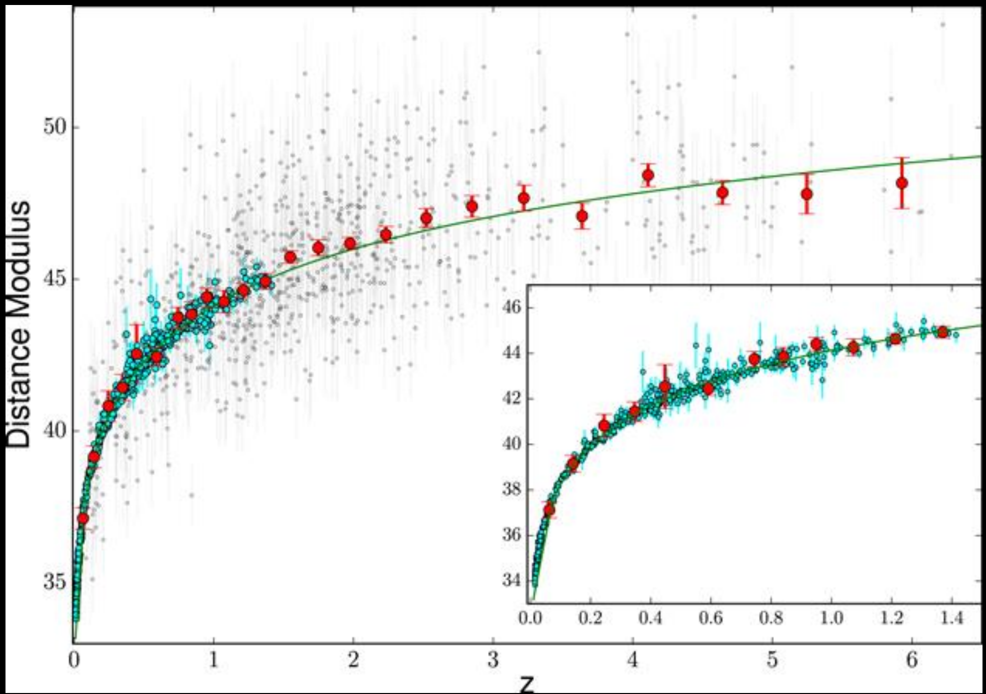

Hubble Diagram for the quasar sample (gray points) and supernovae (cyan points)

G. Risaliti & E. Lusso, 2015, ApJ, 815, 33

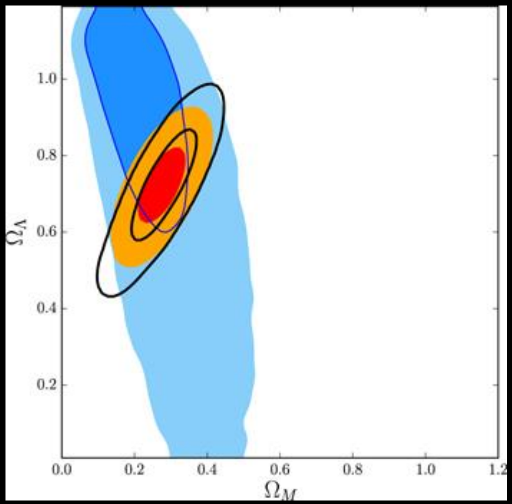

68% and 95% contours for and , assuming a standard ΛCDM model, as derived from our analysis of the Hubble diagram of quasars (blue), from the SNe sample (empty black), and from a joint fit (orange–red).

1138 quasars with X-ray measurements and SDSS:

(1) nonlinear relation between X-ray and UV luminosities up to z ≈ 6

(2) Hubble diagram for quasars up to z ≈ 6, which is well matched to that of supernovae in the common z = 0–1.4 redshift interval and extends the test of the cosmological model up to z~6

(3) powerful tool for estimating cosmological parameters

What's past is prologue; what to come,
In yours and my discharge[1]

[1] W. Shakespeare, 1623, The Tempest, Act 2, Scene 1

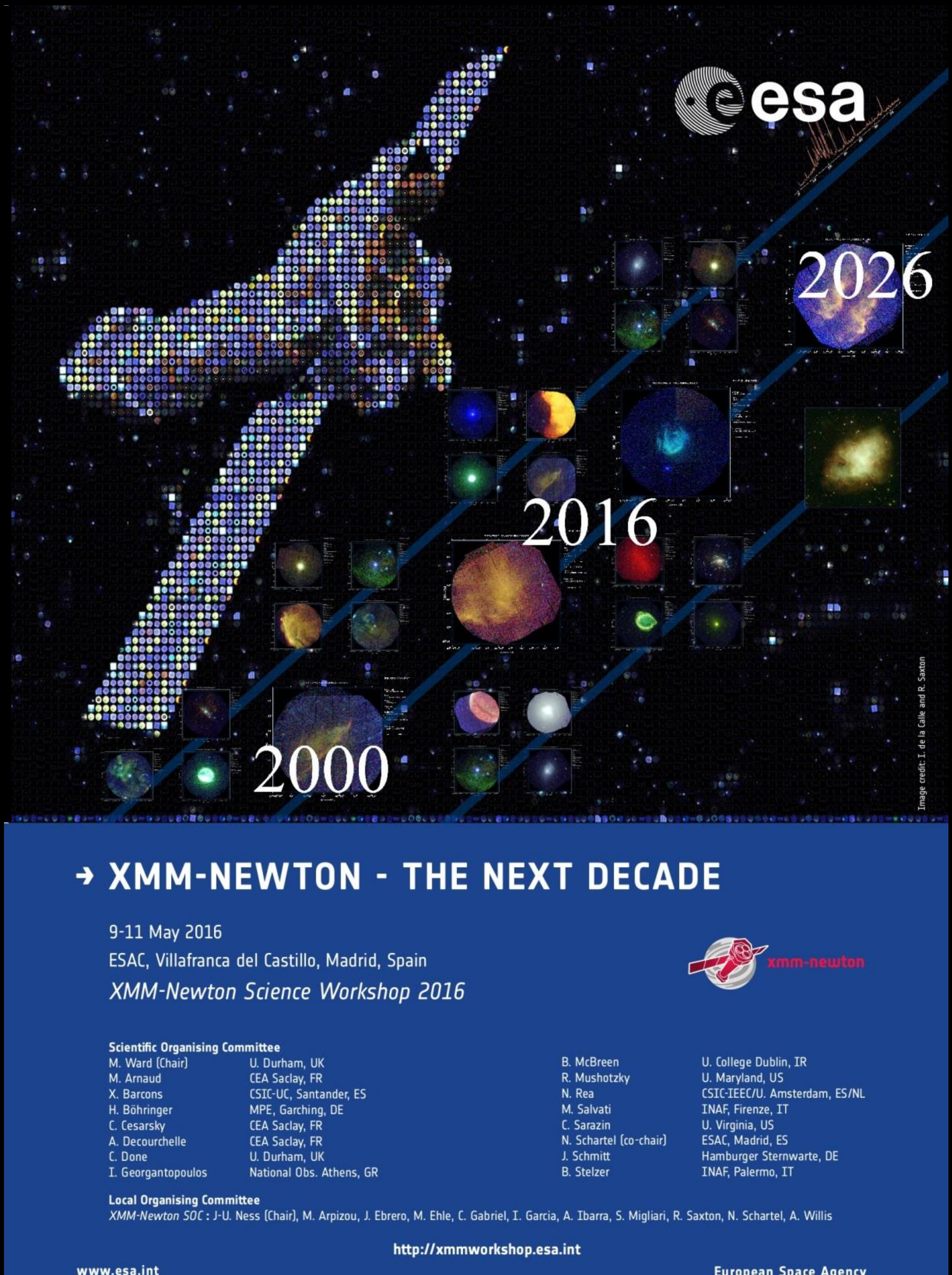

XMM-NEWTON- THE NEXT DECADE

9-11 May 2015

ESAC, Madrid, Spain